

On the topological surface states of the intrinsic magnetic topological insulator Mn-Bi-Te family

Yuan Wang¹, Xiao-Ming Ma¹, Zhanyang Hao¹, Yongqing Cai¹, Hongtao Rong¹, Fayuan Zhang¹, Weizhao Chen¹, Chengcheng Zhang¹, Junhao Lin¹, Yue Zhao^{1#}, Chang Liu^{1#}, Qihang Liu^{1#}, and Chaoyu Chen^{1#}

¹ Shenzhen Institute for Quantum Science and Engineering (SIQSE) and Department of Physics, Southern University of Science and Technology (SUSTech), Shenzhen 518055, China.

[#]Correspondence should be addressed to Y.Z. (zhaoy@sustech.edu.cn), C.L. (liuc@sustech.edu.cn), Q.L. (liuqh@sustech.edu.cn) and C.C. (chency@sustech.edu.cn)

ABSTRACT

We review recent progress in the electronic structure study of intrinsic magnetic topological insulators $(\text{MnBi}_2\text{Te}_4) \cdot (\text{Bi}_2\text{Te}_3)_n$ ($n = 0, 1, 2, 3$) family. Specifically, we focus on the ubiquitously (nearly) gapless behavior of topological surface state Dirac cone observed by photoemission spectroscopy, even though a large Dirac gap is expected because of surface ferromagnetic order. The dichotomy between experiment and theory concerning this gap behavior is perhaps the most critical and puzzling question in this frontier. We discuss various proposals accounting for the lack of magnetic effect on the topological surface state Dirac cone, which are mainly categorized into two pictures, magnetic reconfiguration, and topological surface state redistribution. Band engineering towards opening a magnetic gap of topological surface states provides great opportunities to realize quantized topological transport and axion electrodynamics at higher temperatures.

Keywords: Intrinsic magnetic topological insulator, topological surface states, magnetic gap, magnetic reconfiguration, topological surface state redistribution, van der Waals spacing expansion.

1. Introduction

Magnetism has been used and studied over millennia. Yet, this branch of physics keeps flourishing in recent years with emerging states of magnetic matters such as quantum spin liquid [1,2] and two-dimensional (2D) magnets [3,4]. By comparison, the first two decades of the new millennium embraced the triumph of topological states of matter, which has revolutionized our knowledge of crystalline materials by introducing topological invariants to categorize their electronic structure [5,6]. In 2007, the realization of the quantum spin Hall effect (QSHE) based on a 2D HgTe/CdTe quantum well [7,8] opened a new era of exploring topological phases and materials in condensed matter. Electronically, this QSH state is insulating with a bulk gap separating the conduction and

valence bands but has a pair of one-dimensional (1D) conducting edge states. These 1D topological edge states are protected by time-reversal symmetry, wherein elastic backscattering by nonmagnetic impurities is forbidden, holding potential for dissipationless spintronics. The QSHE state can be classified by a type of topological invariant called Z_2 invariant [9] and is now recognized as the first example of 2D time-reversal invariant topological insulator (TI) with $Z_2 = 1$. Z_2 classification can be generalized to three-dimensional (3D) to describe “weak” and “strong” 3D TIs [10]. A 3D strong TI has ubiquitous, gapless topological surface state (TSS) with helical spin texture due to the spin-momentum locking. In 2008, 3D TI was first realized based on Bi-Sb alloys [11] with multiple TSSs crossing the Fermi level 5 times. Up to now, there have been hundreds of materials predicted as 3D strong TI [12-14] and dozens of them have been experimentally verified, usually through direct observation of their TSS Dirac cone by angle-resolved photoemission spectroscopy (ARPES) [15-17]. Among them, the most representing one is Bi_2Se_3 family of materials [18-21] found in 2009. Bi_2Se_3 family is now considered as the “hydrogen atom” of topological materials due to its simple and elegant electronic structure. It is a semiconductor with a bulk gap of ~ 0.3 eV, among the few with sizable bulk gap to manifest surface state transport. It has only one TSS Dirac cone at the Brillouin zone (BZ) center, with the Dirac point located close to the middle of bulk gap. It consists of -Se-Bi-Se-Bi-Se- quintuple layers (QLs) stacking along c axis and bound by van der Waals (vdW) interaction, easy for device fabrication and epitaxial growth. Importantly, it is chemically stable and the robustness of TSS when exposed to ambient environment has been firmly established [22]. These excellent properties distinguish Bi_2Se_3 family from others for the exploration of novel topological effects. Particularly, the quantum anomalous Hall effect (QAHE), a time-reversal-symmetry-breaking version of QSHE, was predicted in 2010 [23] and then realized in 2013 [24] based on magnetically doped films of this family (Fig. 1).

Our story of topological states of matter has reached a point where this rising star meets a classic field of physics, magnetism. However, this is not their first rendezvous. Back in 1980, the quantum Hall effect (QHE) was observed from a 2D electron gas system subjected to a strong magnetic field [25]. This phenomenon was later explained theoretically as a topological property of the occupied bands in BZ [26]. In the current context, we can call the QHE the first topological insulator ever found, classified by a time-reversal-symmetry-breaking topological invariant called Chern number C (originally the well-known Thouless–Kohmoto–Nightingale–Nijs invariant [26]). The applied magnetic field in QHE can be replaced by the intrinsic magnetization of the material, leading to QAHE. In this regard, QHE and QAHE states are both Chern insulators. In 2D Chern insulators, 1D gapless edge states emerge at the boundary between the Chern insulator and ordinary insulator (vacuum) because of the distinct band topology. Like the 1D helical edge states of QSHE, the 1D chiral edge state in QAHE can propagate along one direction with forbidden backscattering, suitable for developing low-power-consumption electronics without the need for applied magnetic field.

The prediction and realization of QAHE [23,24] represent a breakthrough in fundamental physics, yet much effort is needed toward its practical application. On the one hand, Hall bar devices based on magnetically doped films require sophisticated epitaxial growth and microfabrication procedures that only a few labs in the world can accomplish [24,27-34]. On the other hand, atomic doping brings disorders to the crystal and inhomogeneity to the electronic structure, resulting in much reduced effective exchange gap of the TSS, where the realization temperature was as low as 30 *mK* at first [24] and the current record is 2 *K* [30] after ten years' effort. In this context, intrinsic magnetic TI, which combines magnetic order and band topology in the same material without the need of doping, is highly desired.

In a magnetic TI, while the time-reversal symmetry θ is broken by the magnetic order, its combination with certain magnetic lattice symmetry such as rotation C_n and fractional translation $T_{1/2}$ can retain an equivalent time-reversal symmetry and the system can still be classified by the topological Z_2 invariant. This was first discussed in the theoretical proposal of antiferromagnetic TI (AFM TI) in 2010 [35]. In an AFM TI, both θ and $T_{1/2}$ are broken but the combination $S = \theta T_{1/2}$ is preserved, leading to a topologically nontrivial phase which shares with 3D strong TI the topological Z_2 invariant and quantized magnetoelectric effect. The difference is that, while 3D TIs have symmetry protected gapless TSS at all surfaces, 3D AFM TIs have intrinsically gapped TSS at certain surfaces with broken S symmetry. The gapped TSSs in 3D AFM TIs carry a half-quantized Hall conductivity ($\sigma_{xy} = e^2/2h$), which may aid experimental confirmation of quantized magnetoelectric coupling (Fig. 1). Although with fascinating properties, the material realization of an intrinsic AFM TI was initiated until 2017. First-principles calculation proposed that by inserting MnTe bilayer into the quintuple layer of Bi₂Te₃, the septuple layers of MnBi₂Te₄ host a robust QAH state [36,37]. The material was first experimentally realized with thin films via molecular beam epitaxy [38]. Theoretical works on single crystalline MnBi₂Te₄ were reported in 2019 and revealed its fertile topological states of matter [39-42]. Since the successful preparation of single crystal MnBi₂Te₄, the surge of intrinsic magnetic TI based on MnBi₂Te₄ family of materials started.

Now we know more details concerning the structural, magnetic, and topological aspects of MnBi₂Te₄ AFM TI. Its $R\bar{3}m$ lattice consists of layered -Te-Bi-Te-Mn-Te-Bi-Te- units (SL) stacking along the *c* axis and the layers are bounded by vdW force [43,44]. In the ground state below $T_N \sim 24.6$ *K*, Mn ions ($S = 5/2$ of 2+ valence) with a large magnetic moment of $\sim 5 \mu_B$ form a ferromagnetic (FM) layer with moments pointing out-of-plane. These FM layers couple each other in an AFM way along the *c* axis [45,46] (A-type AFM). The bulk gap is around 220 *meV* from calculation [42] but only ~ 130 *meV* as directly observed by ARPES [47-49]. At the natural cleavage plane (0001), the TSS gap of ~ 88 *meV* at the Dirac point is expected due to the S breaking [39-42]. This sizable TSS gap is the key ingredient enabling the observation of exotic phenomena such as quantized magnetoelectric coupling [35,50,51], axion electrodynamics [52,53], QAHE

[24,27-34,54] and chiral Majorana fermions [55-58] at much higher temperatures. In fact, quantum transport experiments have revealed the existence of a 2D Chern insulator with QAHE observed at 1.4 K based on 5 SLs [59], and the characteristics of an axion insulator state based on 6 SLs [60], both at zero magnetic field. Under a perpendicular magnetic field (15 T), characteristics of high-Chern-number quantum Hall effect without Landau levels contributed by dissipationless chiral edge states are observed, indicating a well-defined Chern insulator state with $C = 2$ (9, 10 SLs) [61]. Its intralayer FM and interlayer AFM configuration exhibits layer Hall effect in which electrons from the top and bottom layers deflect in opposite directions due to the layer-locked Berry curvature, resulting in the characteristic of the axion insulator state (6 SLs) [62]. In addition to these experimental observations, it is further shown by theory that manipulating its magnetic and structural configuration can give rise to many new topological states. For example, the flat Chern band in twisted bilayer MnBi_2Te_4 may boost fractional Chern insulator and $p + ip$ topological superconductor [63]; changing the stacking order between MnBi_2Te_4 SL and Bi_2Te_3 QL may lead to novel states such as QSHE insulator with and without time-reversal symmetry [64]; magnetic ground states other than A-type AFM may lead to different phases such as Weyl semimetal [65,66] and higher-order topological Möbius insulator [67]. These predictions (Fig. 1) certainly deserve further experimental efforts.

There have been several reviews/perspectives on this intrinsic magnetic TI family [68-72], with distinct emphases on theoretical, computational and transport study, respectively. In this review, we focus on the electronic structure of $(\text{MnBi}_2\text{Te}_4) \cdot (\text{Bi}_2\text{Te}_3)_n$ ($n = 0, 1, 2, 3$) family, which has long been a subject of much debate. We will first review the ARPES observation of ubiquitously (nearly) gapless behavior of TSS Dirac cone from MnBi_2Te_4 and MnBi_2Te_4 SL termination, as well as the band hybridization features from Bi_2Te_3 QL terminations. While the significantly reduced TSS gap size of MnBi_2Te_4 termination deviates from that obtained by first-principles calculations, it is not against the relatively low temperature for the observation of QAHE, suggesting that the effective magnetic moments for the TSS may be diminished. There are also experimental evidence suggesting the robust A-type AFM order at the topmost SL layers from magnetic force microscopy (MFM), polar reflective magnetic circular dichroism (RMCD) and X-ray magnetic circular/linear dichroism (XMCD/XMLD) measurements. Furthermore, the magnetic splitting of certain bulk quasi-2D bands seems to validate the effect of magnetic order on the low-energy band structure. Bearing these established experimental results in mind, we then discuss the validity of possible scenarios proposed to account for the (nearly) gapless TSS from MnBi_2Te_4 termination, such as surface magnetic reconstruction, TSS redistribution, defect and self-doping effects, etc. Future band engineering towards opening a magnetic gap at the TSS Dirac point via approaches such as magnetic manipulation, element substitution, chemical potential and material optimization is proposed, which would provide great opportunities to for the realization of QAHE and topological magnetoelectric effect at higher temperatures.

2. Ubiquitously gapless TSSs

Due to the S breaking at the natural cleavage plane (0001), below $T_N \sim 24.6$ K AFM TI MnBi_2Te_4 is expected to show a magnetic gap ~ 88 meV at the Dirac point of TSS [39-42]. Earlier ARPES investigations on the single crystals reported gapped TSS behavior with a Dirac gap ranging from 70 meV to 200 meV [42,73,74], in line with the theoretical prediction. However, the photon-energy dependent gap size indicates its bulk nature rather than a surface origin. Indeed, our systematic photon-energy-dependent ARPES measurements show that the bulk gap separating the bulk valence and conduction bands varies from 130 meV to 200 meV from bulk BZ Γ to Z [47]. Astonishingly, the TSS Dirac cone remains gapless below or above $T_N \sim 24.6$ K, as first reported by our group (data shown in Fig. 2a) and others [47-49]. Such observations of (nearly) gapless TSS Dirac cone on MnBi_2Te_4 (0001) surface below and above the AFM order temperature have been further repeated [75-79]. To date, there have been extensive efforts to explain the origin of this gapless behavior, which will be reviewed in the following sections.

The striking violation against the theoretical picture has inspired intensive ARPES measurements extended to the AFM heterostructure members of this family, i.e. MnBi_4Te_7 consisting of alternating SL and QL sequence and $\text{MnBi}_6\text{Te}_{10}$ consisting of alternating SL and two QLs sequence [44,80]. The enlarged distance between SLs in MnBi_4Te_7 and $\text{MnBi}_6\text{Te}_{10}$ reduces the AFM exchange interaction. Consequently, MnBi_4Te_7 has an AFM ground state with $T_N \sim 13$ K, while $\text{MnBi}_6\text{Te}_{10}$ is AFM below $T_N \sim 10.7$ K. [81-84]. Due to the vdW interaction between SLs and QLs, MnBi_4Te_7 has two natural cleavage planes (SL and QL terminations) while $\text{MnBi}_6\text{Te}_{10}$ has three (SL, QL, and double QL terminations). Since the intralayer FM order comes from Mn residing in the central layer of SL, one would expect magnetic gap opening from SL termination and gapless TSS from QL and double QL terminations. However, similar to the case of MnBi_2Te_4 (0001) surface, all the SL terminations from MnBi_4Te_7 [49,75,85,86] and $\text{MnBi}_6\text{Te}_{10}$ [75,83,84,87] show (nearly) gapless TSS Dirac cone as presented in Fig. 2b and c. These results suggest that the (nearly) gapless behavior of the TSS Dirac cone is ubiquitous for all the SL terminations of $(\text{MnBi}_2\text{Te}_4)_n(\text{Bi}_2\text{Te}_3)_m$ ($n = 0, 1, 2$).

It is also interesting to look at the TSS behavior from QL and double QL terminations. Both QL terminations from MnBi_4Te_7 (Fig. 2b, right) and $\text{MnBi}_6\text{Te}_{10}$ (Fig. 2c, middle) present similar features for the TSS. First of all, the TSS Dirac point is buried inside the bulk valence band region as indicated by blue arrows. Secondly, an apparent gap is opened at the upper TSS Dirac cone due to its hybridization with one neighboring bulk valence band. Thirdly, below this hybridization gap, the residual TSS and bulk valence band compose a Rashba-split band (RSB) feature, with the new RSB Dirac point coming from the original TSS Dirac point. Lastly and more importantly, there appears a new band inside the hybridization gap, with its top touching the upper part of the gapped TSS, forming a new gapless Dirac cone. This in-gap state extends from the new Dirac point down to the valence band region, resulting in the generally gapless surface and bulk spectra. The

appearance of this new in-gap Dirac cone is intriguing. Based on the above band features, a TSS-RSB hybridization picture has been proposed to explain the complicated band features from both SL and QL terminations [84]. Combining circular dichroism ARPES and first-principles calculations, the existence of RSB and its hybridization with TSS are firmly established by works from several groups [73,79,84,86,88]. The TSS-RSB hybridization can be simulated in a tight-binding simulation. By tuning the hybridization strength, the QL ARPES spectra can be reproduced. According to the simulation, the new in-gap Dirac cone indeed comes from the original bulk RSB (see Fig. 4b-d in ref. [84]). This hybridization picture can also reproduce well the SL ARPES spectra and potentially explain the puzzling gapless behavior of TSS Dirac point, which will be discussed in detail in the following section. For the double QL termination of $\text{MnBi}_6\text{Te}_{10}$, similar band hybridization features are observed (Fig. 2c, right), but the hybridization gap is too narrow to distinguish any in-gap state.

3. Key properties related to the TSS gap

Since its first observation, attempts had been made to explain the gapless behavior of TSS Dirac point from SL in AFM phase with S breaking [47-49]. Before going to the bewildering variety of proposals, we would like to mention the key properties established by various experimental probes, which are closely related to the gapless/gapped behavior of TSS at the SL.

The first one comes from the realization of QAHE observed at 1.4 K based on 5 SLs of MnBi_2Te_4 [59], as shown in Fig. 3a. This strongly suggests the existence of 2D Chern insulator state with gapped TSS. By fitting the Arrhenius plot of longitudinal resistance R_{xx} as a function of $1/T$, the energy gap of the thermally activated charge transport can be obtained as $\Delta E = 0.64 \text{ meV}$ at zero-field [59]. This energy scale characterizes the minimum energy required to excite an electron from the surface valence to the surface conduction band, two orders of magnitude smaller than the exchange gap predicted [42]. Consequently, the gapless behavior of TSS observed by ARPES may just represent the resolving power of the instrument, and the TSS gap could still exist but be smaller than the energy resolution (typically $> 1 \text{ meV}$). The TSS gap size from ARPES measurements varies from being diminished [47,48], to $\sim 10 \text{ meV}$ [49] or even larger, with strong sample and spatial dependence [89,90]. The above observations suggest that the gapless behavior of TSS Dirac point at SL termination at AFM phase is unlikely symmetry enforced. It is worth noting that, according to the theoretical definition of AFM TI, the TSS is protected in a weaker sense than the 3D strong TI, as it is generally not stable to disorder [35].

The second key property is the robust A-type AFM order at the surface SL layers as evidenced by measurements using MFM [91] and other techniques. Fig. 3b shows the MFM image taken after field cooling at 0.6 T , with the tip polarized by a magnetic field -0.3 T perpendicular to the sample surface. Clear contrast in the image illustrates several domains, where the magnetic signal changes

its sign when crossing the domain walls. If the magnetic moment on the tip is reversed by a magnetic field of $0.3 T$, all the domains and domain walls change their contrast. Further analysis of the screening effect from fractional QL impurity phases supports the persistence of uniaxial A-type spin order at the top SL layers. One may wonder if the robustness of A-AFM at the top SL layers is also sample dependent. It is thus important to note that other techniques, such as polar reflective magnetic circular dichroism (RMCD) [92] and X-ray magnetic circular/linear dichroism (XMCD/XMLD) [42,45,89,93-95] spectroscopies, also give strong evidence for the existence of net out-of-plane magnetic moments at the sample surfaces.

Even though the robust A-type AFM order is confirmed, what about its influence on the low-energy electronic structure? The (nearly) gapless behavior and its weak temperature dependence across the magnetic transition suggest a negligible effect of the magnetic order on the TSS. However, there are other bands close to the Fermi level which are surprisingly affected by the magnetic order. As exemplified in Fig. 3c by the bulk conduction bands labeled as $CB1_a$ and $CB1_b$, at high temperatures they merge into one band $CB1$, while their splitting starts when the temperature decreased to T_N and reaches $\sim 35 - 45 meV$ below $10 K$ [48,49,96]. It is further reported that $CB2$ also shows a Rashba-like feature and band splitting below T_N [76]. These results firmly demonstrated the third key property of $MnBi_2Te_4$, i.e. the coupling between AFM order and the low-energy bands.

The fourth one comes from a material point of view concerning the disorders typically present in transition metal chalcogenides. In $MnBi_2Te_4$ family, various types of disorders, such as Bi_{Te} antisites (i.e. Bi atoms at the Te sites) located in the surface layer, Mn_{Bi} substitutions (Mn-Bi intermixing) in the second and central atomic layer, and Mn vacancies (V_{Mn}) are observed by combining many experimental tools such as scanning transmission electron microscope (STEM) imaging, scanning tunneling microscopy (STM) imaging, single-crystal X-ray diffraction (SCXRD), energy dispersive x-ray (EDX) analysis in scanning electron microscope (SEM) [45,46,74,90,97-105] and even density functional theory (DFT) calculations [106]. We will show in the next section that certain types of disorders may strongly affect the magnetic response of TSS.

4. Magnetic reconfiguration to explain the (nearly) gapless TSSs

The (nearly) gapless behavior of TSS and its weak temperature dependence across the AFM order lead to a natural speculation of surface magnetic reconstruction. Deviations from the A-AFMz type (Fig. 4a), such as disordered magnetic structure (Fig. 4b), G-AFM with intralayer and interlayer AFM (Fig. 4c) and AFMx with FM in-plane moments (Fig. 4d), are considered in calculations [47,65,67,107]. As shown in Fig. 4b-d, all the three deviations can lead to gapless TSS. Since it remains as a technical challenge to determine the magnetic structure for the topmost SL, it would be insightful to examine the specific features from ARPES measured spectra corresponding to the various magnetic structure. As shown in the right panel of Fig. 4d, for A-AFMx, the net magnetic

moments break the in-plane rotation symmetry and leads to TSS constant energy contour (CEC) with only mirror symmetry. Further consideration of spin texture even shows the mirror symmetry breaking [107]. For G-AFM, the double-sized unit cell in the AFM phase may leads to in-plane band folding feature compared to the paramagnetic phase. For the disordered case, the lack of any oriented moment would retain the sixfold rotation symmetry of TSS CEC, while for the A-AFMz, the net out-of-plane moments in the top SL layer coupled to the TSS will break the sixfold rotation symmetry and leave only threefold rotation symmetry. Further ARPES studies with three components (P_x, P_y, P_z) spin resolution and ultrahigh energy, momentum resolution are highly encouraged to distinguish the above features.

Another type of magnetic reconfiguration is the formation of domains and domain walls illustrated in Fig. 4e (left panel [28]). The existence of magnetic domain walls in MnBi_2Te_4 surface has been observed experimentally [91,108]. Gapless chiral boundary modes are topologically protected to exist in the presence of opposing magnetic domains [109], which is confirmed by the first-principles-based tight-binding model (Fig. 4d, right panel [110]). Note that this edge mode is strictly gapless, while the TSS gap size in MnBi_2Te_4 shows sample and spatial dependence [89,90]. It is further argued that, as the typical domain size is $\sim 10 \mu\text{m}$, the tiny contribution of chiral edge states at domain walls is insufficient to explain the gapless topological surface states [91].

One more sophisticated ferrimagnetic structure has been experimentally observed [100,101] and employed to account for the much reduced TSS gap [97]. As shown in Fig. 4f, the Mn-Bi intermixing could introduce Mn_{Bi} defects in the second and sixth atomic layers counting from the surface, with its moments antiparallel to that of the central Mn layer. Due to the predominant localization of TSS density of states to the Te-Bi-Te layer, the moments of Mn_{Bi} defects counteract that from the central Mn layer, leading to TSS gap reduction. The inhomogeneity of Mn_{Bi} defects could explain the sample and spatial dependence of TSS gap size, suggesting that improving the sample crystalline quality to suppress the Mn-Bi intermixing is a crucial task for the near future study [97]. However, to really correlate the Mn_{Bi} defect density to the TSS gap size, one needs to perform *in situ* ARPES and STM measurements for the same region of the sample surface, which is hardly feasible considering that these two techniques have “field of view” with orders of magnitude difference.

It is also reasonable to check the effective coupling between Mn d orbitals contributing magnetism and Bi/Te p orbital related to the TSS. According to a resonant photoemission study [49], the Mn $3d$ states are mainly located 4 eV below the Fermi level (Fig. 4g), negligible in the energy range where nontrivial topology arises, indicating weak coupling between magnetism and TSS. This weak $p - d$ hybridization scenario seems to contradict the observation of magnetism-induced conduction band splitting as discussed in section III. Based on the above analyses, there remain plenty of challenging experiments to perform, microscopically or spectroscopically, to determine the topmost SL magnetic structure accounting for the (nearly) gapless TSS.

5. TSS redistribution to explain its (nearly) gapless behavior

In this section we introduce the TSS redistribution picture which could attribute the (nearly) gapless TSS Dirac point to the extended TSS distribution from the topmost SL to the layers beneath, leading to compromised effective magnetic moments the TSS can feel. The compensation of the effective magnetic moments relies on the fact that the topmost SL and the second SL have antiparallel and comparable moments, meaning that this TSS redistribution picture is only applicable to MnBi_2Te_4 but not the heterostructure members containing nonmagnetic QLs. However, the potential driving force to redistribute the TSS, such as band hybridization, vdW spacing expansion, or charge/defect effect, maybe generally exist in all the members of this family. In the following, we briefly introduce these mechanisms.

Based on the observation of hybridization between the TSS and a pair of RSBs, A TSS-RSB hybridization picture has been proposed [84] to explain the origin of sophisticated band structure for both QL and SL terminations in this material family (see details in section II). Specifically for SL as shown in Fig. 5a, tight-binding model simulation reveals that the TSS Dirac cone has a bulk origin. This inspires a TSS redistribution picture to account for the lack of magnetic effect on TSS in MnBi_2Te_4 . As schematically illustrated in Fig. 5b, in an *ideal* case the TSS predominantly locates on the topmost SL. In the A-AFM configuration, the effective magnetic moments for the TSS are approximately equal to the net FM moments from one SL, which is large enough to open a sizable TSS Dirac gap as expected. In the *actual* case, the TSS distribution extends to the second SL. The interlayer AFM order results in zero net magnetization for the top two SLs and consequently compensated effective magnetic moments for the TSS. In an extreme situation where the top two SLs equally share 50% of TSS localization, gapless TSS appears regardless of the robust surface A-AFM order and its coupling to the band structure. Based on this TSS redistribution picture, a sizeable TSS magnetic gap can be expected if the magnetic compensation effect is eliminated, say, in a FM ground state. This *expected* case will be discussed in the next section.

Such TSS redistribution picture has been indeed supported by numerous model analysis and calculations based on distinct approaches. Starting from a 3D Hamiltonian for bulk MnBi_2Te_4 and taking into account the spatial profile of the bulk magnetization, an effective model for the TSS has been derived [111]. This model suggests that the diminished surface gap may be caused by a much smaller and more localized intralayer ferromagnetic order and the fact that the surface states are mainly embedded in the first two SLs from the terminating surface (Fig. 5c). To be specific, by using the envelope function the penetration depth of TSS is calculated as $\sim 16.2 \text{ \AA}$, larger than the thickness of one SL ($\sim 13.7 \text{ \AA}$). This is in agreement with the results obtained by *ab initio* calculations, which present the spatial charge distribution of the TSS Dirac state at equilibrium

structure and for vdW spacing between the first and second SL expanded by 15.3% (Fig. 5e from ref. [89]). With increasing vdW spacing, the TSS is found to shift its dominant occupation from the top SL to the second SL, resulting in reduced effective moments. The TSS Dirac gap is found to decrease and vanish at 15.3% expansion. As the vdW spacing modulation is likely to occur in both magnetic and nonmagnetic vdW TIs, a general three-Dirac-fermion approach can be developed [112] to describe the TSS behavior. As shown in Fig. 5f, the three-Dirac-fermion refers to three TSS Dirac cones located at the top surface of the topmost SL/QL (D_1), the bottom surface of the topmost SL/QL (D_2) and the top surface of the second SL/QL (D_3), respectively. Their coupling is tuned by coupling energies Δ_{12} and Δ_{23} , with the latter being dependent on the topmost interlayer vdW spacing d . Remarkably, unexpected gapless TSS Dirac cones are found to arise due to d expansion, when the total Chern number of the system changes by 1 in this expansion process. It should be emphasized that, in this three-Dirac-fermion approach, the gapless point is topologically protected and comes from the competition between the Zeeman coupling and the Dirac fermion coupling. Such vdW spacing expansion may be introduced by mechanical cleavage process [22,113] before ARPES and STM measurements, yet it is missing the direct evidence from atomic layer resolved probes such as STEM.

Excess surface charge is found to affect the distribution of TSS in a top/bottom cone-dependent manner [90]. Obviously, the smallest gap values should be achieved when the top and bottom TSS cones are mostly and independently located in two adjacent SLs, as they experience an exchange field of the opposite sign ($q = -0.045e_0$ in Fig. 5d). Furthermore, from an *ab initio* calculation, cation co-antisites Mn_{Bi} and Bi_{Mn} (extra Bi replacing Mn) can push the TSS charge toward the second SL, the top SL's influence on the magnetic gap is reduced while the second SL influence is enhanced simultaneously (Fig. 5g) [114], resulting in compensated effective magnetic moments and reduce TSS magnetic gap. It is noted that the existence of excess charge and Mn-Bi intermixing defects is well established in this material family.

6. Perspectives to open the TSS magnetic gap

In the context of TSS redistribution picture, gapless TSS comes from compensated magnetic moments as a nature of the A-AFM order. Assuming an FM background, no compensation exists no matter how the TSS redistributes. This indeed offers a great chance to realize a sizeable TSS gap through magnetic engineering based on $MnBi_2Te_4$. In fact, large amount of Sb substitution in the Bi sites can indeed transform the $MnBi_2Te_4$ ground state from AFM to FM or ferrimagnetic order [98,100,115-117]. The TSS band structure study by ARPES, however, is difficult due to the heavy hole doping induced by Sb substitution. It is worth noting that with small amount of Sb doping, we have observed a TSS gap opening in $MnBi_2Te_4$ samples which stay at the AFM phase. Surprisingly

this TSS gap size is proportional to the doping level and carrier density, allowing a continuous tunability of gap size [118]. However, this TSS gap is independent of the AFM- paramagnetic transition, with the origin of gap remaining to be investigated.

Another way to realize the FM ground state is through heterostructure engineering. As mentioned in section II, in $(\text{MnBi}_2\text{Te}_4) \cdot (\text{Bi}_2\text{Te}_3)_n$ ($n = 0, 1, 2, 3$) family the interlayer AFM coupling between the FM SLs can be reduced by QL spacing. In fact, with 3 QLs spacing ($n = 3$), $\text{MnBi}_8\text{Te}_{13}$ develops a long-range FM order below $T_C = 10.5 \text{ K}$ [119]. This provides a valuable chance to realize the magnetic gap in TSS from SL termination. High-quality $\text{MnBi}_8\text{Te}_{13}$ single crystals are grown and characterized through structural, magnetic, transport and electronic structure studies [120]. Its crystal structure shown in Fig. 6a was obtained from SCXRD and powder XRD refinement. The temperature-dependent anisotropic magnetic susceptibility (Fig. 6b) shows Curie-Weiss (CW) behavior above 150 K (inset) with the characteristic temperature $\theta_{CW} = 12.5 \text{ K}$ and 10.5 K for $H \parallel c$ and $H \parallel ab$, respectively. The larger bifurcation between zero-field cooling (ZFC) and field cooling (FC) magnetization and magnetic hysteresis loop (Fig. 6c) indicate an easy axis along the c -axis and an Ising-type exchange interaction between adjacent Mn layers. These properties suggest a FM order with an out-of-plane magnetic moment configuration in $\text{MnBi}_8\text{Te}_{13}$.

The heterostructure lattice of $\text{MnBi}_8\text{Te}_{13}$ naturally yields four types of terminations by cleaving the single crystal perpendicular to the c axis, namely, SL, QL, double QL and triple QL terminations. A spatial-resolved ARPES with a Laser beam spot around $5 \mu\text{m}$ was employed to resolve the intrinsic surface band structure from these four distinct terminations and the results are shown here in Fig. 6e-h. We start with those 3 nonmagnetic QL terminations and find very similar TSS-RSB hybridization features as we discovered from QL and double QL terminations of $\text{MnBi}_6\text{Te}_{10}$ (Fig. 2c [84]), while the triple QL termination shows a TSS Dirac cone resembling that of Bi_2Te_3 . Emphasizing was put on the SL termination and a clear gap can be found at the TSS Dirac point as indicated by the black arrow in Fig. 6e. The gap size is extracted by fitting the energy distribution curves (EDCs) using multiple Lorentzian peaks. The fitting yields TSS Dirac gap $\sim 28 \text{ meV}$ at 7 K . Furthermore, this gap size exhibits a monotonical decrease with increasing temperature (Fig. 6d) and gap closing at 11 K , right above T_C , establishing an FM-induced Dirac-point gap in the SL termination. Although TSS gaps have been observed in other members of this materials family and doped TIs, their magnetic origin remains controversial with particularly the lack of clear temperature dependence [47,48,75,84,121]. Consequently, this observation—that a TSS Dirac cone gap decreases monotonically with increasing temperature and closes right at T_C , forming a gapless Dirac cone—represent the direct evidence of TSSs gapped by the magnetic order among all known magnetic topological materials. It is still more desirable to realize the magnetic gap of TSSs in MnBi_2Te_4 rather than its heterostructure cousins as the latter present uncontrollable terminations with different magnetism from the exfoliation process. The realization of the TSS magnetic gap in

FM $\text{MnBi}_8\text{Te}_{13}$ seems to be consistent with the TSS redistribution picture.

We have discussed several possible microscopic mechanisms of TSS in two aspects, i.e., magnetic configuration (such as disordered magnetic structure and A-AFMx with FM in-plane moments) and TSS redistribution (such as TSS-RSB hybridization, vdW spacing expansion, excess surface charge, and cation co-antistite effect). It should be noted that, to reach any of these situations, an energy barrier needs to be overcome due to its deviation from the bulk ground states. Hence, a natural question rises up: why these situations would occur? Does it occasionally exist in Mn-Bi-Te family or some deep mechanism lead to it? From the perspective of energy competition, a more general self-doping scenario in real samples had been proposed as the essential force that may drive to such situations based on Koopmans' theorem [122]. For the gapped TSS, the energy level of the conduction band minimum is higher than that for the case of the gapless Dirac point. According to Koopmans' theorem, an electronic self-doping would naturally save energy for the gapless TSS. Once such energy gain overwhelms the energy barrier of any situation to redistribute the TSS or magnetization, the gapless behavior of TSS emerges. In this sense, the self-doping may be the deep origin of nearly gapless TSS, while the TSS redistribution or magnetic reconfiguration serves as the intermediate. In this view, the emergence of the magnetic gap of $\text{MnBi}_8\text{Te}_{13}$ could also be understood. Instead of locating at the surface SL that contributes to TSS, most of the self-doped electrons enter the bulk QL bands, thus suppressing the gapless transition of TSS [122]. Therefore, to open the TSS magnetic gap it is favorable to recover its charge neutrality via doping or material optimizing.

Despite the remaining puzzles of the microscopic mechanism of TSS, there are currently experimental advances that may be informative. Related to the vdW gap mechanism, point contact tunneling spectroscopy on MnBi_2Te_4 observed the signature of the TSS gap, which indicates that a moderate pressure on the surface may deduce the vdW gap expansion to restore the effective magnetic moments for TSS [123]. Related to the excess surface charge and antisite effect, improving the crystalline quality is a direct way to eliminate such effects. Recent efforts in growing MnBi_2Te_4 single crystals using chemical-vapor-transport (CVT) methods [124,125] have reported higher quality samples marked with higher Mn occupancy on the Mn site, slightly higher Mn_{Bi} antisites, smaller carrier concentration, and a Fermi level closer to the Dirac point, yielding highest mobility of $2500 \text{ cm}^2\text{V}^{-1}\text{s}^{-1}$ in MnBi_2Te_4 devices [124]. ARPES measurement with ultrahigh energy and momentum resolution, as in the previous studies [47-49,118,120], is called for the exploration of spectroscopic signature of coupling between the FM order and TSS, such as magnetic gap opening and sixfold rotation symmetry breaking [112,126]. Quantum transport measurement is highly expected based on CVT single crystals for quantized conductivity at higher temperature.

ACKNOWLEDGEMENTS

This work is supported by the National Natural Science Foundation of China (NSFC) (Grants No. 12074163), Guangdong Basic and Applied Basic Research Foundation (Grants No. 2022B1515020046 and No. 2021B1515130007), the Guangdong Innovative and Entrepreneurial Research Team Program (Grant No. 2019ZT08C044), Shenzhen Science and Technology Program (Grant No. KQTD20190929173815000). C.C. acknowledges the assistance of SUSTech Core Research Facilities.

- [1] L. Savary & L. Balents. Quantum spin liquids: a review. *Rep Prog Phys* **80**, 016502, doi:10.1088/0034-4885/80/1/016502 (2017).
- [2] Yi Zhou, Kazushi Kanoda & Tai-Kai Ng. Quantum spin liquid states. *Reviews of Modern Physics* **89**, doi:10.1103/RevModPhys.89.025003 (2017).
- [3] C. Gong, L. Li, Z. Li, H. Ji, A. Stern, Y. Xia, T. Cao, W. Bao, C. Wang, Y. Wang, Z. Q. Qiu, R. J. Cava, S. G. Louie, J. Xia & X. Zhang. Discovery of intrinsic ferromagnetism in two-dimensional van der Waals crystals. *Nature* **546**, 265-269, doi:10.1038/nature22060 (2017).
- [4] Bevin Huang, Genevieve Clark, Efrén Navarro-Moratalla, Dahlia R. Klein, Ran Cheng, Kyle L. Seyler, Ding Zhong, Emma Schmidgall, Michael A. McGuire, David H. Cobden, Wang Yao, Di Xiao, Pablo Jarillo-Herrero & Xiaodong Xu. Layer-dependent ferromagnetism in a van der Waals crystal down to the monolayer limit. *Nature* **546**, 270, doi:10.1038/nature22391 (2017).
- [5] M. Z. Hasan & C. L. Kane. Colloquium: Topological insulators. *Reviews of Modern Physics* **82**, 3045 (2010).
- [6] Xiao-Liang Qi & Shou-Cheng Zhang. Topological insulators and superconductors. *Reviews of Modern Physics* **83**, 1057-1110 (2011).
- [7] B. A. Bernevig, T. L. Hughes & S. C. Zhang. Quantum spin Hall effect and topological phase transition in HgTe quantum wells. *Science* **314**, 1757-1761, doi:DOI 10.1126/science.1133734 (2006).
- [8] M. König, S. Wiedmann, C. Brune, A. Roth, H. Buhmann, L. W. Molenkamp, X. L. Qi & S. C. Zhang. Quantum spin hall insulator state in HgTe quantum wells. *Science* **318**, 766-770, doi:DOI 10.1126/science.1148047 (2007).
- [9] C. L. Kane & E. J. Mele. Z₂ topological order and the quantum spin Hall effect. *Physical Review Letters* **95**, 146802, doi:10.1103/PhysRevLett.95.146802 (2005).
- [10] L. Fu, C. L. Kane & E. J. Mele. Topological insulators in three dimensions. *Physical Review Letters* **98**, - (2007).
- [11] D. Hsieh, D. Qian, L. Wray, Y. Xia, Y. S. Hor, R. J. Cava & M. Z. Hasan. A topological Dirac insulator in a quantum spin Hall phase. *Nature* **452**, 970-974 (2008).
- [12] F. Tang, H. C. Po, A. Vishwanath & X. Wan. Comprehensive search for topological materials using symmetry indicators. *Nature* **566**, 486-489, doi:10.1038/s41586-019-0937-5 (2019).
- [13] M. G. Vergniory, L. Elcoro, C. Felser, N. Regnault, B. A. Bernevig & Z. Wang. A complete catalogue of high-quality topological materials. *Nature* **566**, 480-485, doi:10.1038/s41586-019-0954-4 (2019).
- [14] T. Zhang, Y. Jiang, Z. Song, H. Huang, Y. He, Z. Fang, H. Weng & C. Fang. Catalogue of topological electronic materials. *Nature* **566**, 475-479, doi:10.1038/s41586-019-0944-6 (2019).
- [15] 刘畅 & 刘祥瑞. 强三维拓扑绝缘体与磁性拓扑绝缘体的角分辨光电子能谱学研究进展. *物理学报* **68**, 227901, doi:- 10.7498/aps.68.20191450 (2019).
- [16] Yoichi Ando. Topological Insulator Materials. *Journal of the Physical Society of Japan* **82**, doi:10.7566/jpsj.82.102001 (2013).
- [17] Jonathan A. Sobota, Yu He & Zhi-Xun Shen. Angle-resolved photoemission studies of quantum materials. *Reviews of Modern Physics* **93**, 025006,

- doi:10.1103/RevModPhys.93.025006 (2021).
- [18] Y. L. Chen, J. G. Analytis, J. H. Chu, Z. K. Liu, S. K. Mo, X. L. Qi, H. J. Zhang, D. H. Lu, X. Dai, Z. Fang, S. C. Zhang, I. R. Fisher, Z. Hussain & Z. X. Shen. Experimental Realization of a Three-Dimensional Topological Insulator, Bi₂Te₃. *Science* **325**, 178-181 (2009).
- [19] D. Hsieh, Y. Xia, D. Qian, L. Wray, J. H. Dil, F. Meier, J. Osterwalder, L. Patthey, J. G. Checkelsky, N. P. Ong, A. V. Fedorov, H. Lin, A. Bansil, D. Grauer, Y. S. Hor, R. J. Cava & M. Z. Hasan. A tunable topological insulator in the spin helical Dirac transport regime. *Nature* **460**, 1101-U1159 (2009).
- [20] Y. Xia, D. Qian, D. Hsieh, L. Wray, A. Pal, H. Lin, A. Bansil, D. Grauer, Y. S. Hor, R. J. Cava & M. Z. Hasan. Observation of a large-gap topological-insulator class with a single Dirac cone on the surface. *Nature Physics* **5**, 398-402 (2009).
- [21] H. J. Zhang, C. X. Liu, X. L. Qi, X. Dai, Z. Fang & S. C. Zhang. Topological insulators in Bi₂Se₃, Bi₂Te₃ and Sb₂Te₃ with a single Dirac cone on the surface. *Nature Physics* **5**, 438-442 (2009).
- [22] Chaoyu Chen, Shaolong He, Hongming Weng, Wentao Zhang, Lin Zhao, Haiyun Liu, Xiaowen Jia, Daixiang Mou, Shanyu Liu, Junfeng He, Yingying Peng, Ya Feng, Zhuojin Xie, Guodong Liu, Xiaoli Dong, Jun Zhang, Xiaoyang Wang, Qinjun Peng, Zhimin Wang, Shenjin Zhang, Feng Yang, Chuangtian Chen, Zuyan Xu, Xi Dai, Zhong Fang & X. J. Zhou. Robustness of topological order and formation of quantum well states in topological insulators exposed to ambient environment. *Proceedings of the National Academy of Sciences* **109**, 3694-3698, doi:10.1073/pnas.1115555109 (2012).
- [23] Rui Yu, Wei Zhang, Hai-Jun Zhang, Shou-Cheng Zhang, Xi Dai & Zhong Fang. Quantized Anomalous Hall Effect in Magnetic Topological Insulators. *Science* **329**, 61-64, doi:10.1126/science.1187485 (2010).
- [24] Cui-Zu Chang, Jinsong Zhang, Xiao Feng, Jie Shen, Zuocheng Zhang, Minghua Guo, Kang Li, Yunbo Ou, Pang Wei, Li-Li Wang, Zhong-Qing Ji, Yang Feng, Shuaihua Ji, Xi Chen, Jinfeng Jia, Xi Dai, Zhong Fang, Shou-Cheng Zhang, Ke He, Yayu Wang, Li Lu, Xu-Cun Ma & Qi-Kun Xue. Experimental Observation of the Quantum Anomalous Hall Effect in a Magnetic Topological Insulator. *Science* **340**, 167, doi:10.1126/science.1234414 (2013).
- [25] K. Vonklitzing, G. Dorda & M. Pepper. New Method for High-Accuracy Determination of the Fine-Structure Constant Based on Quantized Hall Resistance. *Physical Review Letters* **45**, 494-497 (1980).
- [26] D. J. Thouless, M. Kohmoto, M. P. Nightingale & M. den Nijs. Quantized Hall Conductance in a Two-Dimensional Periodic Potential. *Physical Review Letters* **49**, 405-408, doi:10.1103/PhysRevLett.49.405 (1982).
- [27] M. Mogi, Y. Okamura, M. Kawamura, R. Yoshimi, K. Yasuda, A. Tsukazaki, K. S. Takahashi, T. Morimoto, N. Nagaosa, M. Kawasaki, Y. Takahashi & Y. Tokura. Experimental signature of the parity anomaly in a semi-magnetic topological insulator. *Nature Physics*, doi:10.1038/s41567-021-01490-y (2022).
- [28] K. Yasuda, M. Mogi, R. Yoshimi, A. Tsukazaki, K. S. Takahashi, M. Kawasaki, F. Kagawa & Y. Tokura. Quantized chiral edge conduction on domain walls of a magnetic topological insulator. *Science* **358**, 1311-1314, doi:doi:10.1126/science.aan5991 (2017).
- [29] Masataka Mogi, Minoru Kawamura, Atsushi Tsukazaki, Ryutaro Yoshimi, Kei S. Takahashi, Masashi Kawasaki & Yoshinori Tokura. Tailoring tricolor structure of magnetic topological

- insulator for robust axion insulator. *Science Advances* **3**, eaao1669, doi:10.1126/sciadv.aao1669 (2017).
- [30] M. Mogi, R. Yoshimi, A. Tsukazaki, K. Yasuda, Y. Kozuka, K. S. Takahashi, M. Kawasaki & Y. Tokura. Magnetic modulation doping in topological insulators toward higher-temperature quantum anomalous Hall effect. *Applied Physics Letters* **107**, 182401, doi:10.1063/1.4935075 (2015).
- [31] C. Z. Chang, W. Zhao, D. Y. Kim, H. Zhang, B. A. Assaf, D. Heiman, S. C. Zhang, C. Liu, M. H. Chan & J. S. Moodera. High-precision realization of robust quantum anomalous Hall state in a hard ferromagnetic topological insulator. *Nat Mater* **14**, 473-477, doi:10.1038/nmat4204 (2015).
- [32] A. J. Bestwick, E. J. Fox, X. Kou, L. Pan, K. L. Wang & D. Goldhaber-Gordon. Precise Quantization of the Anomalous Hall Effect near Zero Magnetic Field. *Phys Rev Lett* **114**, 187201, doi:10.1103/PhysRevLett.114.187201 (2015).
- [33] X. Kou, S. T. Guo, Y. Fan, L. Pan, M. Lang, Y. Jiang, Q. Shao, T. Nie, K. Murata, J. Tang, Y. Wang, L. He, T. K. Lee, W. L. Lee & K. L. Wang. Scale-invariant quantum anomalous Hall effect in magnetic topological insulators beyond the two-dimensional limit. *Phys Rev Lett* **113**, 137201, doi:10.1103/PhysRevLett.113.137201 (2014).
- [34] J. G. Checkelsky, R. Yoshimi, A. Tsukazaki, K. S. Takahashi, Y. Kozuka, J. Falson, M. Kawasaki & Y. Tokura. Trajectory of the anomalous Hall effect towards the quantized state in a ferromagnetic topological insulator. *Nature Physics* **10**, 731-736, doi:10.1038/nphys3053 (2014).
- [35] Roger S. K. Mong, Andrew M. Essin & Joel E. Moore. Antiferromagnetic topological insulators. *Physical Review B* **81**, doi:10.1103/PhysRevB.81.245209 (2010).
- [36] M. M. Otrokov, T. V. Menshchikova, M. G. Vergniory, I. P. Rusinov, A. Yu Vyazovskaya, Yu M. Koroteev, G. Bihlmayer, A. Ernst, P. M. Echenique, A. Arnau & E. V. Chulkov. Highly-ordered wide bandgap materials for quantized anomalous Hall and magnetoelectric effects. *2D Materials* **4**, doi:10.1088/2053-1583/aa6bec (2017).
- [37] M. M. Otrokov, T. V. Menshchikova, I. P. Rusinov, M. G. Vergniory, V. M. Kuznetsov & E. V. Chulkov. Magnetic extension as an efficient method for realizing the quantum anomalous hall state in topological insulators. *JETP Letters* **105**, 297-302, doi:10.1134/s0021364017050113 (2017).
- [38] Yan Gong, Jingwen Guo, Jiaheng Li, Kejing Zhu, Menghan Liao, Xiaozhi Liu, Qinghua Zhang, Lin Gu, Lin Tang, Xiao Feng, Ding Zhang, Wei Li, Canli Song, Lili Wang, Pu Yu, Xi Chen, Yayu Wang, Hong Yao, Wenhui Duan, Yong Xu, Shou-Cheng Zhang, Xucun Ma, Qi-Kun Xue & Ke He. Experimental Realization of an Intrinsic Magnetic Topological Insulator. *Chinese Physics Letters* **36**, doi:10.1088/0256-307x/36/7/076801 (2019).
- [39] D. Zhang, M. Shi, T. Zhu, D. Xing, H. Zhang & J. Wang. Topological Axion States in the Magnetic Insulator MnBi₂Te₄ with the Quantized Magnetoelectric Effect. *Phys Rev Lett* **122**, 206401, doi:10.1103/PhysRevLett.122.206401 (2019).
- [40] M. M. Otrokov, I. P. Rusinov, M. Blanco-Rey, M. Hoffmann, A. Y. Vyazovskaya, S. V. Ereemeev, A. Ernst, P. M. Echenique, A. Arnau & E. V. Chulkov. Unique Thickness-Dependent Properties of the van der Waals Interlayer Antiferromagnet MnBi₂Te₄ Films. *Phys Rev Lett* **122**, 107202, doi:10.1103/PhysRevLett.122.107202 (2019).
- [41] Jiaheng Li, Yang Li, Shiqiao Du, Zun Wang, Bing-Lin Gu, Shou-Cheng Zhang, Ke He,

- Wenhui Duan & Yong Xu. Intrinsic magnetic topological insulators in van der Waals layered MnBi₂Te₄-family materials. *Science Advances* **5**, eaaw5685, doi:10.1126/sciadv.aaw5685 (2019).
- [42] M. M. Otrokov, Klimovskikh, I., H. Bentmann, D. Estyunin, A. Zeugner, Z. S. Aliev, S. Gass, A. U. B. Wolter, A. V. Koroleva, A. M. Shikin, M. Blanco-Rey, M. Hoffmann, I. P. Rusinov, A. Y. Vyazovskaya, S. V. Eremeev, Y. M. Koroteev, V. M. Kuznetsov, F. Freyse, J. Sanchez-Barriga, I. R. Amiraslanov, M. B. Babanly, N. T. Mamedov, N. A. Abdullayev, V. N. Zverev, A. Alfonsov, V. Kataev, B. Buchner, E. F. Schwier, S. Kumar, A. Kimura, L. Petaccia, G. Di Santo, R. C. Vidal, S. Schatz, K. Kissner, M. Unzelmann, C. H. Min, S. Moser, T. R. F. Peixoto, F. Reinert, A. Ernst, P. M. Echenique, A. Isaeva & E. V. Chulkov. Prediction and observation of an antiferromagnetic topological insulator. *Nature* **576**, 416-422, doi:10.1038/s41586-019-1840-9 (2019).
- [43] Dong Sun Lee, Tae-Hoon Kim, Cheol-Hee Park, Chan-Yeup Chung, Young Soo Lim, Won-Seon Seo & Hyung-Ho Park. Crystal structure, properties and nanostructuring of a new layered chalcogenide semiconductor, Bi₂MnTe₄. *CrystEngComm* **15**, doi:10.1039/c3ce40643a (2013).
- [44] Ziya S. Aliev, Imamaddin R. Amiraslanov, Daria I. Nasonova, Andrei V. Shevelkov, Nadir A. Abdullayev, Zakir A. Jahangirli, Elnur N. Orujlu, Mikhail M. Otrokov, Nazim T. Mamedov, Mahammad B. Babanly & Evgueni V. Chulkov. Novel ternary layered manganese bismuth tellurides of the MnTe-Bi₂Te₃ system: Synthesis and crystal structure. *Journal of Alloys and Compounds* **789**, 443-450, doi:10.1016/j.jallcom.2019.03.030 (2019).
- [45] Alexander Zeugner, Frederik Nietschke, Anja U. B. Wolter, Sebastian Gaß, Raphael C. Vidal, Thiago R. F. Peixoto, Darius Pohl, Christine Damm, Axel Lubk, Richard Hentrich, Simon K. Moser, Celso Fornari, Chul Hee Min, Sonja Schatz, Katharina Kißner, Maximilian Unzelmann, Martin Kaiser, Francesco Scaravaggi, Bernd Rellinghaus, Kornelius Nielsch, Christian Hess, Bernd Büchner, Friedrich Reinert, Hendrik Bentmann, Oliver Oeckler, Thomas Doert, Michael Ruck & Anna Isaeva. Chemical Aspects of the Candidate Antiferromagnetic Topological Insulator MnBi₂Te₄. *Chemistry of Materials* **31**, 2795-2806, doi:10.1021/acs.chemmater.8b05017 (2019).
- [46] J. Q. Yan, Q. Zhang, T. Heitmann, Zengle Huang, K. Y. Chen, J. G. Cheng, Weida Wu, D. Vaknin, B. C. Sales & R. J. McQueeney. Crystal growth and magnetic structure of MnBi₂Te₄. *Physical Review Materials* **3**, 064202, doi:10.1103/PhysRevMaterials.3.064202 (2019).
- [47] Yu-Jie Hao, Pengfei Liu, Yue Feng, Xiao-Ming Ma, Eike F. Schwier, Masashi Arita, Shiv Kumar, Chaowei Hu, Rui'e Lu, Meng Zeng, Yuan Wang, Zhanyang Hao, Hong-Yi Sun, Ke Zhang, Jiawei Mei, Ni Ni, Liusuo Wu, Kenya Shimada, Chaoyu Chen, Qihang Liu & Chang Liu. Gapless Surface Dirac Cone in Antiferromagnetic Topological Insulator MnBi₂Te₄. *Physical Review X* **9**, 041038, doi:10.1103/PhysRevX.9.041038 (2019).
- [48] Y. J Chen, L. X Xu, J. H Li, Y. W Li, H. Y Wang, C. F Zhang, H. Li, Y. Wu, A. J Liang, C. Chen, S. W Jung, C. Cacho, Y. H Mao, S. Liu, M. X Wang, Y. F Guo, Y. Xu, Z. K Liu, L. X Yang & Y. L Chen. Topological Electronic Structure and Its Temperature Evolution in Antiferromagnetic Topological Insulator MnBi₂Te₄. *Physical Review X* **9**, 041040, doi:10.1103/PhysRevX.9.041040 (2019).
- [49] Hang Li, Shun-Ye Gao, Shao-Feng Duan, Yuan-Feng Xu, Ke-Jia Zhu, Shang-Jie Tian, Jia-Cheng Gao, Wen-Hui Fan, Zhi-Cheng Rao, Jie-Rui Huang, Jia-Jun Li, Da-Yu Yan, Zheng-

- Tai Liu, Wan-Ling Liu, Yao-Bo Huang, Yu-Liang Li, Yi Liu, Guo-Bin Zhang, Peng Zhang, Takeshi Kondo, Shik Shin, He-Chang Lei, You-Guo Shi, Wen-Tao Zhang, Hong-Ming Weng, Tian Qian & Hong Ding. Dirac Surface States in Intrinsic Magnetic Topological Insulators EuSn_2As_2 and $\text{MnBi}_2\text{nTe}_{3n+1}$. *Physical Review X* **9**, 041039, doi:10.1103/PhysRevX.9.041039 (2019).
- [50] Xiao-Liang Qi, Taylor L. Hughes & Shou-Cheng Zhang. Topological field theory of time-reversal invariant insulators. *Physical Review B* **78**, doi:10.1103/PhysRevB.78.195424 (2008).
- [51] A. M. Essin, J. E. Moore & D. Vanderbilt. Magnetoelectric polarizability and axion electrodynamics in crystalline insulators. *Phys Rev Lett* **102**, 146805, doi:10.1103/PhysRevLett.102.146805 (2009).
- [52] Rundong Li, Jing Wang, Xiao-Liang Qi & Shou-Cheng Zhang. Dynamical axion field in topological magnetic insulators. *Nature Physics* **6**, 284-288 (2010).
- [53] Jing Wang, Biao Lian & Shou-Cheng Zhang. Dynamical axion field in a magnetic topological insulator superlattice. *Physical Review B* **93**, doi:10.1103/PhysRevB.93.045115 (2016).
- [54] Huixia Fu, Chao-Xing Liu & Binghai Yan. Exchange bias and quantum anomalous normal Hall effect in the $\text{MnBi}_2\text{Te}_4/\text{CrI}_3$ heterostructure. *Science Advances* **6**, eaaz0948, doi:10.1126/sciadv.aaz0948 (2020).
- [55] Zhenyu Wang, Jorge Olivares Rodriguez, Lin Jiao, Sean Howard, Martin Graham, G. D. Gu, Taylor L. Hughes, Dirk K. Morr & Vidya Madhavan. Evidence for dispersing 1D Majorana channels in an iron-based superconductor. *Science* **367**, 104, doi:10.1126/science.aaw8419 (2020).
- [56] Alexandra Palacio-Morales, Eric Mascot, Sagen Cocklin, Howon Kim, Stephan Rachel, Dirk K. Morr & Roland Wiesendanger. Atomic-scale interface engineering of Majorana edge modes in a 2D magnet-superconductor hybrid system. *Science Advances* **5**, eaav6600, doi:10.1126/sciadv.aav6600 (2019).
- [57] K. Yasuda, M. Mogi, R. Yoshimi, A. Tsukazaki, K. S. Takahashi, M. Kawasaki, F. Kagawa & Y. Tokura. Quantized chiral edge conduction on domain walls of a magnetic topological insulator. *Science* **358**, 1311, doi:10.1126/science.aan5991 (2017).
- [58] Qing Lin He, Lei Pan, Alexander L. Stern, Edward C. Burks, Xiaoyu Che, Gen Yin, Jing Wang, Biao Lian, Quan Zhou, Eun Sang Choi, Koichi Murata, Xufeng Kou, Zhijie Chen, Tianxiao Nie, Qiming Shao, Yabin Fan, Shou-Cheng Zhang, Kai Liu, Jing Xia & Kang L. Wang. Chiral Majorana fermion modes in a quantum anomalous Hall insulator-superconductor structure. *Science* **357**, 294, doi:10.1126/science.aag2792 (2017).
- [59] Yujun Deng, Yijun Yu, Meng Zhu Shi, Zhongxun Guo, Zihan Xu, Jing Wang, Xian Hui Chen & Yuanbo Zhang. Quantum anomalous Hall effect in intrinsic magnetic topological insulator MnBi_2Te_4 . *Science* **367**, 895-900, doi:10.1126/science.aax8156 (2020).
- [60] Chang Liu, Yongchao Wang, Hao Li, Yang Wu, Yaoxin Li, Jiaheng Li, Ke He, Yong Xu, Jinsong Zhang & Yayu Wang. Robust axion insulator and Chern insulator phases in a two-dimensional antiferromagnetic topological insulator. *Nature Materials* **19**, 522-527, doi:10.1038/s41563-019-0573-3 (2020).
- [61] Jun Ge, Yanzhao Liu, Jiaheng Li, Hao Li, Tianchuang Luo, Yang Wu, Yong Xu & Jian Wang. High-Chern-number and high-temperature quantum Hall effect without Landau levels.

- National Science Review* **7**, 1280-1287, doi:10.1093/nsr/nwaa089 (2020).
- [62] A. Gao, Y. F. Liu, C. Hu, J. X. Qiu, C. Tzschaschel, B. Ghosh, S. C. Ho, D. Berube, R. Chen, H. Sun, Z. Zhang, X. Y. Zhang, Y. X. Wang, N. Wang, Z. Huang, C. Felser, A. Agarwal, T. Ding, H. J. Tien, A. Akey, J. Gardener, B. Singh, K. Watanabe, T. Taniguchi, K. S. Burch, D. C. Bell, B. B. Zhou, W. Gao, H. Z. Lu, A. Bansil, H. Lin, T. R. Chang, L. Fu, Q. Ma, N. Ni & S. Y. Xu. Layer Hall effect in a 2D topological axion antiferromagnet. *Nature* **595**, 521-525, doi:10.1038/s41586-021-03679-w (2021).
- [63] B. Lian, Z. Liu, Y. Zhang & J. Wang. Flat Chern Band from Twisted Bilayer MnBi₂Te₄. *Phys Rev Lett* **124**, 126402, doi:10.1103/PhysRevLett.124.126402 (2020).
- [64] H. Sun, B. Xia, Z. Chen, Y. Zhang, P. Liu, Q. Yao, H. Tang, Y. Zhao, H. Xu & Q. Liu. Rational Design Principles of the Quantum Anomalous Hall Effect in Superlatticelike Magnetic Topological Insulators. *Phys Rev Lett* **123**, 096401, doi:10.1103/PhysRevLett.123.096401 (2019).
- [65] Jiaheng Li, Chong Wang, Zetao Zhang, Bing-Lin Gu, Wenhui Duan & Yong Xu. Magnetically controllable topological quantum phase transitions in the antiferromagnetic topological insulator MnBi₂Te₄. *Physical Review B* **100**, doi:10.1103/PhysRevB.100.121103 (2019).
- [66] Sugata Chowdhury, Kevin F. Garrity & Francesca Tavazza. Prediction of Weyl semimetal and antiferromagnetic topological insulator phases in Bi₂MnSe₄. *npj Computational Materials* **5**, doi:10.1038/s41524-019-0168-1 (2019).
- [67] R. X. Zhang, F. Wu & S. Das Sarma. Mobius Insulator and Higher-Order Topology in MnBi_{2n}Te_{3n+1}. *Phys Rev Lett* **124**, 136407, doi:10.1103/PhysRevLett.124.136407 (2020).
- [68] 占国慧, 王怀强, 张海军. 反铁磁拓扑绝缘体与轴子绝缘体-MnBi₂Te₄ 系列磁性体系的研究进展. *物理* **49**, 817-827, doi:10.7693/wl20201203 (2020).
- [69] Ke He. MnBi₂Te₄-family intrinsic magnetic topological materials. *npj Quantum Materials* **5**, 90, doi:10.1038/s41535-020-00291-5 (2020).
- [70] Yang Li & Yong Xu. First-principles discovery of novel quantum physics and materials: From theory to experiment. *Computational Materials Science* **190**, 110262, doi:10.1016/j.commatsci.2020.110262 (2021).
- [71] P. Wang, J. Ge, J. Li, Y. Liu, Y. Xu & J. Wang. Intrinsic magnetic topological insulators. *Innovation* **2**, 100098, doi:10.1016/j.xinn.2021.100098 (2021).
- [72] Yufei Zhao & Qihang Liu. Routes to realize the axion-insulator phase in MnBi₂Te₄(Bi₂Te₃)_n family. *Applied Physics Letters* **119**, doi:10.1063/5.0059447 (2021).
- [73] R. C. Vidal, H. Bentmann, T. R. F. Peixoto, A. Zeugner, S. Moser, C. H. Min, S. Schatz, K. Kißner, M. Ünzelmann, C. I. Fornari, H. B. Vasili, M. Valvidares, K. Sakamoto, D. Mondal, J. Fujii, I. Vobornik, S. Jung, C. Cacho, T. K. Kim, R. J. Koch, C. Jozwiak, A. Bostwick, J. D. Denlinger, E. Rotenberg, J. Buck, M. Hoesch, F. Diekmann, S. Rohlf, M. Källäne, K. Rossnagel, M. M. Otrokov, E. V. Chulkov, M. Ruck, A. Isaeva & F. Reinert. Surface states and Rashba-type spin polarization in antiferromagnetic MnBi₂Te₄ (0001). *Physical Review B* **100**, doi:10.1103/PhysRevB.100.121104 (2019).
- [74] Seng Huat Lee, Yanglin Zhu, Yu Wang, Leixin Miao, Timothy Pillsbury, Hemian Yi, Susan Kempinger, Jin Hu, Colin A. Heikes, P. Quarterman, William Ratcliff, Julie A. Borchers, Heda Zhang, Xianglin Ke, David Graf, Nasim Alem, Cui-Zu Chang, Nitin Samarth & Zhiqiang Mao. Spin scattering and noncollinear spin structure-induced intrinsic anomalous Hall

- effect in antiferromagnetic topological insulator MnBi₂Te₄. *Physical Review Research* **1**, doi:10.1103/PhysRevResearch.1.012011 (2019).
- [75] Yong Hu, Lixuan Xu, Mengzhu Shi, Aiyun Luo, Shuting Peng, Z. Y. Wang, J. J. Ying, T. Wu, Z. K. Liu, C. F. Zhang, Y. L. Chen, G. Xu, X. H. Chen & J. F. He. Universal gapless Dirac cone and tunable topological states in (MnBi₂Te₄)_m(Bi₂Te₃)_n heterostructures. *Physical Review B* **101** (2020).
- [76] D. Nevola, H. X. Li, J. Q. Yan, R. G. Moore, H. N. Lee, H. Miao & P. D. Johnson. Coexistence of Surface Ferromagnetism and a Gapless Topological State in MnBi₂Te₄. *Phys Rev Lett* **125**, 117205, doi:10.1103/PhysRevLett.125.117205 (2020).
- [77] Przemyslaw Swatek, Yun Wu, Lin-Lin Wang, Kyungchan Lee, Benjamin Schruck, Jiaqiang Yan & Adam Kaminski. Gapless Dirac surface states in the antiferromagnetic topological insulator MnBi₂Te₄. *Physical Review B* **101**, doi:10.1103/PhysRevB.101.161109 (2020).
- [78] T. Fukasawa, S. Kusaka, K. Sumida, M. Hashizume, S. Ichinokura, Y. Takeda, S. Ideta, K. Tanaka, R. Shimizu, T. Hitosugi & T. Hirahara. Absence of ferromagnetism in MnBi₂Te₄/Bi₂Te₃ down to 6 K. *Physical Review B* **103**, doi:10.1103/PhysRevB.103.205405 (2021).
- [79] Chenhui Yan, Sebastian Fernandez-Mulligan, Ruobing Mei, Seng Huat Lee, Nikola Protic, Rikuto Fukumori, Binghai Yan, Chaoxing Liu, Zhiqiang Mao & Shuolong Yang. Origins of electronic bands in the antiferromagnetic topological insulator MnBi₂Te₄. *Physical Review B* **104**, doi:10.1103/PhysRevB.104.L041102 (2021).
- [80] J. Wu, F. Liu, C. Liu, Y. Wang, C. Li, Y. Lu, S. Matsuishi & H. Hosono. Toward 2D Magnets in the (MnBi₂ Te₄)(Bi₂ Te₃)_n Bulk Crystal. *Adv Mater* **32**, e2001815, doi:10.1002/adma.202001815 (2020).
- [81] J. Q. Yan, Y. H. Liu, D. S. Parker, Y. Wu, A. A. Aczel, M. Matsuda, M. A. McGuire & B. C. Sales. A-type antiferromagnetic order in MnBi₄Te₇ and MnBi₆Te₁₀ single crystals. *Physical Review Materials* **4**, doi:10.1103/PhysRevMaterials.4.054202 (2020).
- [82] Lei Ding, Chaowei Hu, Feng Ye, Erxi Feng, Ni Ni & Huibo Cao. Crystal and magnetic structures of magnetic topological insulators MnBi₂Te₄ and MnBi₄Te₇. *Physical Review B* **101**, doi:10.1103/PhysRevB.101.020412 (2020).
- [83] Shangjie Tian, Shunye Gao, Simin Nie, Yuting Qian, Chunsheng Gong, Yang Fu, Hang Li, Wenhui Fan, Peng Zhang, Takesh Kondo, Shik Shin, Johan Adell, Hanna Fedderwitz, Hong Ding, Zhijun Wang, Tian Qian & Hechang Lei. Magnetic topological insulator MnBi₆Te₁₀ with a zero-field ferromagnetic state and gapped Dirac surface states. *Physical Review B* **102**, doi:10.1103/PhysRevB.102.035144 (2020).
- [84] Xiao-Ming Ma, Zhongjia Chen, Eike F. Schwier, Yang Zhang, Yu-Jie Hao, Shiv Kumar, Ruie Lu, Jifeng Shao, Yuanjun Jin, Meng Zeng, Xiang-Rui Liu, Zhanyang Hao, Ke Zhang, Wumiti Mansuer, Chunyao Song, Yuan Wang, Boyan Zhao, Cai Liu, Ke Deng, Jiawei Mei, Kenya Shimada, Yue Zhao, Xingjiang Zhou, Bing Shen, Wen Huang, Chang Liu, Hu Xu & Chaoyu Chen. Hybridization-induced gapped and gapless states on the surface of magnetic topological insulators. *Physical Review B* **102**, 245136, doi:10.1103/PhysRevB.102.245136 (2020).
- [85] Xuefeng Wu, Jiayu Li, Xiao-Ming Ma, Yu Zhang, Yuntian Liu, Chun-Sheng Zhou, Jifeng Shao, Qiaoming Wang, Yu-Jie Hao, Yue Feng, Eike F. Schwier, Shiv Kumar, Hongyi Sun, Pengfei Liu, Kenya Shimada, Koji Miyamoto, Taichi Okuda, Kedong Wang, Maohai Xie,

- Chaoyu Chen, Qihang Liu, Chang Liu & Yue Zhao. Distinct Topological Surface States on the Two Terminations of MnBi₄Te₇. *Physical Review X* **10**, 031013, doi:10.1103/PhysRevX.10.031013 (2020).
- [86] R. C. Vidal, H. Bentmann, J. I. Facio, T. Heider, P. Kagerer, C. I. Fornari, T. R. F. Peixoto, T. Figgemeier, S. Jung, C. Cacho, B. Buchner, J. van den Brink, C. M. Schneider, L. Plucinski, E. F. Schwier, K. Shimada, M. Richter, A. Isaeva & F. Reinert. Orbital Complexity in Intrinsic Magnetic Topological Insulators MnBi₄Te₇ and MnBi₆Te₁₀. *Phys Rev Lett* **126**, 176403, doi:10.1103/PhysRevLett.126.176403 (2021).
- [87] Na Hyun Jo, Lin-Lin Wang, Robert-Jan Slager, Jiaqiang Yan, Yun Wu, Kyungchan Lee, Benjamin Schruck, Ashvin Vishwanath & Adam Kaminski. Intrinsic axion insulating behavior in antiferromagnetic MnBi₆Te₁₀. *Physical Review B* **102**, doi:10.1103/PhysRevB.102.045130 (2020).
- [88] A. Liang, C. Chen, H. Zheng, W. Xia, K. Huang, L. Wei, H. Yang, Y. Chen, X. Zhang, X. Xu, M. Wang, Y. Guo, L. Yang, Z. Liu & Y. Chen. Approaching a Minimal Topological Electronic Structure in Antiferromagnetic Topological Insulator MnBi₂Te₄ via Surface Modification. *Nano Lett* **22**, 4307-4314, doi:10.1021/acs.nanolett.1c04930 (2022).
- [89] A. M. Shikin, D. A. Estyunin, Klimovskikh, I. S. O. Filnov, E. F. Schwier, S. Kumar, K. Miyamoto, T. Okuda, A. Kimura, K. Kuroda, K. Yaji, S. Shin, Y. Takeda, Y. Saitoh, Z. S. Aliev, N. T. Mamedov, I. R. Amiraslanov, M. B. Babanly, M. M. Otrokov, S. V. Eremeev & E. V. Chulkov. Nature of the Dirac gap modulation and surface magnetic interaction in axion antiferromagnetic topological insulator MnBi₂Te₄. *Sci Rep* **10**, 13226, doi:10.1038/s41598-020-70089-9 (2020).
- [90] A. M. Shikin, D. A. Estyunin, N. L. Zaitsev, D. Glazkova, I. I. Klimovskikh, S. O. Filnov, A. G. Rybkin, E. F. Schwier, S. Kumar, A. Kimura, N. Mamedov, Z. Aliev, M. B. Babanly, K. Kokh, O. E. Tereshchenko, M. M. Otrokov, E. V. Chulkov, K. A. Zvezdin & A. K. Zvezdin. Sample-dependent Dirac-point gap in MnBi₂Te₄ and its response to applied surface charge: A combined photoemission and ab initio study. *Physical Review B* **104**, doi:10.1103/PhysRevB.104.115168 (2021).
- [91] Paul M Sass, Jinwoong Kim, David Vanderbilt, Jiaqiang Yan & Weida Wu. Robust A-Type Order and Spin-Flop Transition on the Surface of the Antiferromagnetic Topological Insulator MnBi₂Te₄. *Physical Review Letters* **125**, doi:10.1103/PhysRevLett.125.037201 (2020).
- [92] Shiqi Yang, Xiaolong Xu, Yaozheng Zhu, Ruirui Niu, Chunqiang Xu, Yuxuan Peng, Xing Cheng, Xionghui Jia, Yuan Huang, Xiaofeng Xu, Jianming Lu & Yu Ye. Odd-Even Layer-Number Effect and Layer-Dependent Magnetic Phase Diagrams in MnBi₂Te₄. *Physical Review X* **11**, doi:10.1103/PhysRevX.11.011003 (2021).
- [93] P. Kagerer, C. I. Fornari, S. Buchberger, S. L. Morelhão, R. C. Vidal, A. Tcakaev, V. Zabolotnyy, E. Weschke, V. Hinkov, M. Kamp, B. Büchner, A. Isaeva, H. Bentmann & F. Reinert. Molecular beam epitaxy of antiferromagnetic (MnBi₂Te₄)(Bi₂Te₃) thin films on BaF₂ (111). *Journal of Applied Physics* **128**, doi:10.1063/5.0025933 (2020).
- [94] T. Hirahara, M. M. Otrokov, T. T. Sasaki, K. Sumida, Y. Tomohiro, S. Kusaka, Y. Okuyama, S. Ichinokura, M. Kobayashi, Y. Takeda, K. Amemiya, T. Shirasawa, S. Ideta, K. Miyamoto, K. Tanaka, S. Kuroda, T. Okuda, K. Hono, S. V. Eremeev & E. V. Chulkov. Fabrication of a novel magnetic topological heterostructure and temperature evolution of its massive Dirac cone.

- Nat Commun* **11**, 4821, doi:10.1038/s41467-020-18645-9 (2020).
- [95] Raphael C. Vidal, Alexander Zeugner, Jorge I. Facio, Rajyavardhan Ray, M. Hossein Haghighi, Anja U. B Wolter, Laura T. Corredor Bohorquez, Federico Cagliaris, Simon Moser, Tim Figgemeier, Thiago R. F Peixoto, Hari Babu Vasili, Manuel Valvidares, Sungwon Jung, Cephise Cacho, Alexey Alfonsov, Kavita Mehlawat, Vladislav Kataev, Christian Hess, Manuel Richter, Bernd Büchner, Jeroen van den Brink, Michael Ruck, Friedrich Reinert, Hendrik Bentmann & Anna Isaeva. Topological Electronic Structure and Intrinsic Magnetization in MnBi₄Te₇: A Bi₂Te₃ Derivative with a Periodic Mn Sublattice. *Physical Review X* **9**, doi:10.1103/PhysRevX.9.041065 (2019).
- [96] D. A. Estyunin, I. I. Klimovskikh, A. M. Shikin, E. F. Schwier, M. M. Otrokov, A. Kimura, S. Kumar, S. O. Filnov, Z. S. Aliev, M. B. Babanly & E. V. Chulkov. Signatures of temperature driven antiferromagnetic transition in the electronic structure of topological insulator MnBi₂Te₄. *APL Materials* **8**, doi:10.1063/1.5142846 (2020).
- [97] M. Garnica, M. M. Otrokov, P. Casado Aguilar, I. I. Klimovskikh, D. Estyunin, Z. S. Aliev, I. R. Amiraslanov, N. A. Abdullayev, V. N. Zverev, M. B. Babanly, N. T. Mamedov, A. M. Shikin, A. Arnau, A. L. Vázquez de Parga, E. V. Chulkov & R. Miranda. Native point defects and their implications for the Dirac point gap at MnBi₂Te₄(0001). *npj Quantum Materials* **7**, doi:10.1038/s41535-021-00414-6 (2022).
- [98] S. Wimmer, J. Sanchez-Barriga, P. Kuppers, A. Ney, E. Schierle, F. Freyse, O. Caha, J. Michalicka, M. Liebmann, D. Primetzhofer, M. Hoffman, A. Ernst, M. M. Otrokov, G. Bihlmayer, E. Weschke, B. Lake, E. V. Chulkov, M. Morgenstern, G. Bauer, G. Springholz & O. Rader. Mn-Rich MnSb₂Te₄ : A Topological Insulator with Magnetic Gap Closing at High Curie Temperatures of 45-50 K. *Adv Mater* **33**, e2102935, doi:10.1002/adma.202102935 (2021).
- [99] Joanna Sitnicka, Kyungwha Park, Paweł Skupiński, Krzysztof Graszka, Anna Reszka, Kamil Sobczak, Jolanta Borysiuk, Zbigniew Adamus, Mateusz Tokarczyk, Andrei Avdonin, Irina Fedorchenko, Irina Abaloszewa, Sylwia Turczyniak-Surdacka, Natalia Olszowska, Jacek Kołodziej, Bogdan J. Kowalski, Haiming Deng, Marcin Konczykowski, Lia Krusin-Elbaum & Agnieszka Wołoś. Systemic consequences of disorder in magnetically self-organized topological MnBi₂Te₄/(Bi₂Te₃)_n superlattices. *2D Materials* **9**, doi:10.1088/2053-1583/ac3cc6 (2021).
- [100] Yaohua Liu, Lin-Lin Wang, Qiang Zheng, Zengle Huang, Xiaoping Wang, Miaofang Chi, Yan Wu, Bryan C. Chakoumakos, Michael A. McGuire, Brian C. Sales, Weida Wu & Jiaqiang Yan. Site Mixing for Engineering Magnetic Topological Insulators. *Physical Review X* **11**, doi:10.1103/PhysRevX.11.021033 (2021).
- [101] You Lai, Liqin Ke, Jiaqiang Yan, Ross D. McDonald & Robert J. McQueeney. Defect-driven ferrimagnetism and hidden magnetization in MnBi₂Te₄. *Physical Review B* **103**, doi:10.1103/PhysRevB.103.184429 (2021).
- [102] Chaowei Hu, Shang-Wei Lien, Erxi Feng, Scott Mackey, Hung-Ju Tien, Igor I. Mazin, Huibo Cao, Tay-Rong Chang & Ni Ni. Tuning magnetism and band topology through antisite defects in Sb-doped MnBi₄Te₇. *Physical Review B* **104**, doi:10.1103/PhysRevB.104.054422 (2021).
- [103] Y. Yuan, X. Wang, H. Li, J. Li, Y. Ji, Z. Hao, Y. Wu, K. He, Y. Wang, Y. Xu, W. Duan, W. Li & Q. K. Xue. Electronic States and Magnetic Response of MnBi₂Te₄ by Scanning Tunneling

- Microscopy and Spectroscopy. *Nano Lett* **20**, 3271-3277, doi:10.1021/acs.nanolett.0c00031 (2020).
- [104] Zuwei Liang, Aiyun Luo, Mengzhu Shi, Qiang Zhang, Simin Nie, J. J. Ying, J. F. He, Tao Wu, Zhijun Wang, Gang Xu, Zhenyu Wang & X. H. Chen. Mapping Dirac fermions in the intrinsic antiferromagnetic topological insulators $(\text{MnBi}_2\text{Te}_4)(\text{Bi}_2\text{Te}_3)_n$ ($n=0,1$). *Physical Review B* **102**, doi:10.1103/PhysRevB.102.161115 (2020).
- [105] Zengle Huang, Mao-Hua Du, Jiaqiang Yan & Weida Wu. Native defects in antiferromagnetic topological insulator MnBi_2Te_4 . *Physical Review Materials* **4**, doi:10.1103/PhysRevMaterials.4.121202 (2020).
- [106] Mao-Hua Du, Jiaqiang Yan, Valentino R. Cooper & Markus Eisenbach. Tuning Fermi Levels in Intrinsic Antiferromagnetic Topological Insulators MnBi_2Te_4 and MnBi_4Te_7 by Defect Engineering and Chemical Doping. *Advanced Functional Materials* **31**, doi:10.1002/adfm.202006516 (2020).
- [107] Zhilong Yang & Haijun Zhang. Evolution of surface states of antiferromagnetic topological insulator MnBi_2Te_4 with tuning the surface magnetization. *New Journal of Physics* **24**, 073034, doi:10.1088/1367-2630/ac7e64 (2022).
- [108] P. M. Sass, W. Ge, J. Yan, D. Obeysekera, J. J. Yang & W. Wu. Magnetic Imaging of Domain Walls in the Antiferromagnetic Topological Insulator MnBi_2Te_4 . *Nano Lett* **20**, 2609-2614, doi:10.1021/acs.nanolett.0c00114 (2020).
- [109] Yoshinori Tokura, Kenji Yasuda & Atsushi Tsukazaki. Magnetic topological insulators. *Nature Reviews Physics* **1**, 126-143, doi:10.1038/s42254-018-0011-5 (2019).
- [110] Kevin F. Garrity, Sugata Chowdhury & Francesca M. Tavazza. Topological surface states of MnBi_2Te_4 at finite temperatures and at domain walls. *Physical Review Materials* **5**, doi:10.1103/PhysRevMaterials.5.024207 (2021).
- [111] Hai-Peng Sun, C. M. Wang, Song-Bo Zhang, Rui Chen, Yue Zhao, Chang Liu, Qihang Liu, Chaoyu Chen, Hai-Zhou Lu & X. C. Xie. Analytical solution for the surface states of the antiferromagnetic topological insulator MnBi_2Te_4 . *Physical Review B* **102**, 241406(R) doi:10.1103/PhysRevB.102.241406 (2020).
- [112] Dinghui Wang. Three-Dirac-fermion approach to unexpected gapless surface states of van der Waals magnetic topological insulators. *arXiv:2205.08204* (2022).
- [113] T. Menshchikova, S. Ereameev & E. Chulkov. On the origin of two-dimensional electron gas states at the surface of topological insulators. *Jetp Letters* **94**, 106-111, doi:10.1134/s0021364011140104 (2011).
- [114] Hengxin Tan. Distinct magnetic gaps between antiferromagnetic and ferromagnetic orders driven by surface defects in the topological magnet MnBi_2Te_4 . *arXiv:2207.13511* (2022).
- [115] Yangyang Chen, Ya-Wen Chuang, Seng Huat Lee, Yanglin Zhu, Kevin Honz, Yingdong Guan, Yu Wang, Ke Wang, Zhiqiang Mao, Jun Zhu, Colin Heikes, P. Quarterman, Pawel Zajdel, Julie A. Borchers & William Ratcliff. Ferromagnetism in van der Waals compound $\text{MnSb}_{1.8}\text{Bi}_{0.2}\text{Te}_4$. *Physical Review Materials* **4**, doi:10.1103/PhysRevMaterials.4.064411 (2020).
- [116] J. Q. Yan, S. Okamoto, M. A. McGuire, A. F. May, R. J. McQueeney & B. C. Sales. Evolution of structural, magnetic, and transport properties in $\text{MnBi}_{2-x}\text{Sb}_x\text{Te}_4$. *Physical Review B* **100**, doi:10.1103/PhysRevB.100.104409 (2019).

- [117] T. Murakami, Y. Nambu, T. Koretsune, G. Xiangyu, T. Yamamoto, C. M. Brown & H. Kageyama. Realization of interlayer ferromagnetic interaction in MnSb₂Te₄ toward the magnetic Weyl semimetal state. *Phys Rev B* **100**, doi:10.1103/PhysRevB.100.195103 (2019).
- [118] Xiao-Ming Ma, Yufei Zhao, Ke Zhang, Shiv Kumar, Ruie Lu, Jiayu Li, Qiushi Yao, Jifeng Shao, Fuchen Hou, Xuefeng Wu, Meng Zeng, Yu-Jie Hao, Zhanyang Hao, Yuan Wang, Xiang-Rui Liu, Huiwen Shen, Hongyi Sun, Jiawei Mei, Koji Miyamoto, Taichi Okuda, Masashi Arita, Eike F. Schwier, Kenya Shimada, Ke Deng, Cai Liu, Junhao Lin, Yue Zhao, Chaoyu Chen, Qihang Liu & Chang Liu. Realization of a tunable surface Dirac gap in Sb-doped MnBi₂Te₄. *Physical Review B* **103**, L121112, doi:10.1103/PhysRevB.103.L121112 (2021).
- [119] Chaowei Hu, Lei Ding, Kyle N. Gordon, Barun Ghosh, Hung-Ju Tien, Haoxiang Li, A. Garrison Linn, Shang-Wei Lien, Cheng-Yi Huang, Scott Mackey, Jinyu Liu, P. V. Sreenivasa Reddy, Bahadur Singh, Amit Agarwal, Arun Bansil, Miao Song, Dongsheng Li, Su-Yang Xu, Hsin Lin, Huiibo Cao, Tay-Rong Chang, Dan Dessau & Ni Ni. Realization of an intrinsic ferromagnetic topological state in MnBi₈Te₁₃. *Science Advances* **6**, eaba4275, doi:10.1126/sciadv.aba4275 (2020).
- [120] Ruie Lu, Hongyi Sun, Shiv Kumar, Yuan Wang, Mingqiang Gu, Meng Zeng, Yu-Jie Hao, Jiayu Li, Jifeng Shao, Xiao-Ming Ma, Zhanyang Hao, Ke Zhang, Wumiti Mansuer, Jiawei Mei, Yue Zhao, Cai Liu, Ke Deng, Wen Huang, Bing Shen, Kenya Shimada, Eike F Schwier, Chang Liu, Qihang Liu & Chaoyu Chen. Half-Magnetic Topological Insulator with Magnetization-Induced Dirac Gap at a Selected Surface. *Physical Review X* **11**, 011039, doi:10.1103/PhysRevX.11.011039 (2021).
- [121] Lixuan Xu, Yuanhao Mao, Hongyuan Wang, Jiaheng Li, Yujie Chen, Yunyouyou Xia, Yiwei Li, Ding Pei, Jing Zhang, Huijun Zheng, Kui Huang, Chaofan Zhang, Shengtao Cui, Aiji Liang, Wei Xia, Hao Su, Sungwon Jung, Cephise Cacho, Meixiao Wang, Gang Li, Yong Xu, Yanfeng Guo, Lexian Yang, Zhongkai Liu, Yulin Chen & Mianheng Jiang. Persistent surface states with diminishing gap in MnBi₂Te₄/Bi₂Te₃ superlattice antiferromagnetic topological insulator. *Science Bulletin* **65**, 2086-2093, doi:10.1016/j.scib.2020.07.032 (2020).
- [122] Weizhao Chen, Yufei Zhao, Qiushi Yao, Jing Zhang & Qihang Liu. Koopmans' theorem as the mechanism of nearly gapless surface states in self-doped magnetic topological insulators. *Physical Review B* **103**, doi:10.1103/PhysRevB.103.L201102 (2021).
- [123] Hao-Ran Ji, Yan-Zhao Liu, He Wang, Jia-Wei Luo, Jia-Heng Li, Hao Li, Yang Wu, Yong Xu & Jian Wang. Detection of Magnetic Gap in Topological Surface States of MnBi₂Te₄. *Chinese Physics Letters* **38**, doi:10.1088/0256-307x/38/10/107404 (2021).
- [124] Chaowei Hu, Anyuan Gao, Bryan Stephen Berggren, Hong Li, Rafał Kurlito, Dushyant Narayan, Ilija Zeljkovic, Dan Dessau, Suyang Xu & Ni Ni. Growth, characterization, and Chern insulator state in MnBi₂Te₄ via the chemical vapor transport method. *Physical Review Materials* **5**, doi:10.1103/PhysRevMaterials.5.124206 (2021).
- [125] J. Q. Yan, Zengle Huang, Weida Wu & A. F. May. Vapor transport growth of MnBi₂Te₄ and related compounds. *Journal of Alloys and Compounds* **906**, doi:10.1016/j.jallcom.2022.164327 (2022).
- [126] Hengxin Tan. Momentum-inversion symmetry breaking on the Fermi surface of magnetic topological insulators. *arXiv:2205.07343* (2022).

- [127] B. Lian, X. Q. Sun, A. Vaezi, X. L. Qi & S. C. Zhang. Topological quantum computation based on chiral Majorana fermions. *Proc Natl Acad Sci U S A* **115**, 10938-10942, doi:10.1073/pnas.1810003115 (2018).
- [128] First presented by the author in a symposium on February 1st, 2021 in SUSTech, Shenzhen, China

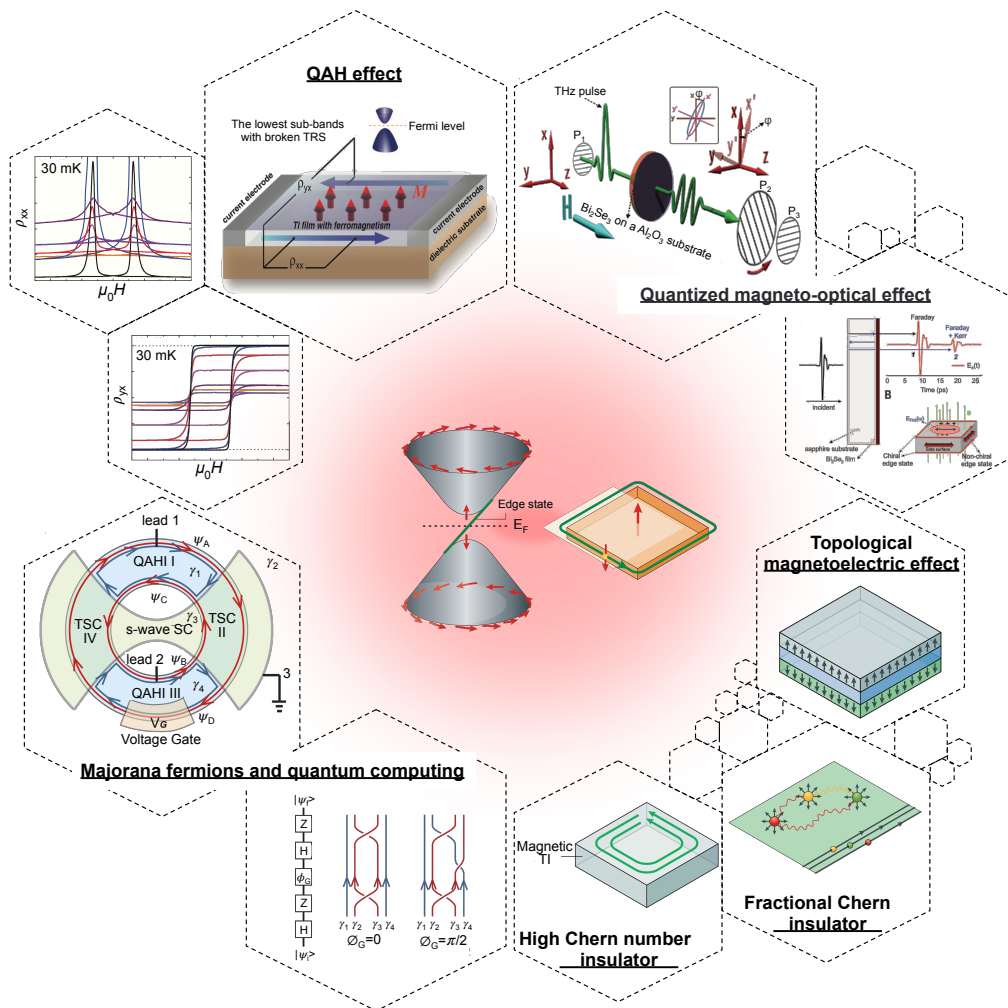


Figure 1. Emergent topological phenomena arising from an intrinsic magnetic TI. The interplay of magnetism and band topology offers a great chance to explore the QAHE previously realized on magnetically doped TI films (adapted from [24]) but now potentially at much higher temperatures, the chiral Majorana fermion at the interface of QAHE state and s-wave superconductor which forms the basis of topological quantum computing (from [127]), quantized magneto-optical effect, topological magnetoelectric effect, fractional Chern insulator, high Chern number insulator and so on (from [109]).

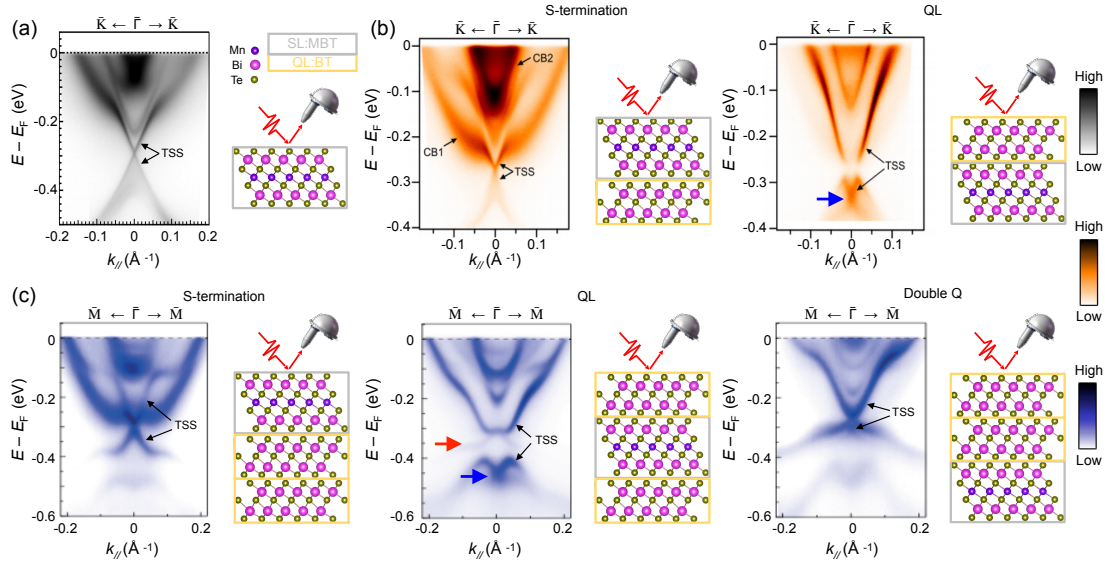


Figure 2. Gapless TSSs from all the terminations of $(\text{MnBi}_2\text{Te}_4) \cdot (\text{Bi}_2\text{Te}_3)_n$ ($n = 0, 1, 2$). (a) Gapless TSS from the (0001) surface of MnBi_2Te_4 , measured at 10 K using photon energy $h\nu = 6.3 \text{ eV}$ [47]. (b) Gapless TSSs from the SL (left) and QL (right) terminations of MnBi_4Te_7 , measured at 11 K using photon energy $h\nu = 6.3 \text{ eV}$ [86]. (c) Gapless TSSs from the SL (left), QL (middle) and double QL (right) terminations of $\text{MnBi}_6\text{Te}_{10}$, measured at 6 K using photon energy $h\nu = 6.994 \text{ eV}$ [75]. Red arrow emphasizes the in-gap states inside the hybridization gap between TSS and bulk valence band while blue arrow indicates the TSS Dirac point.

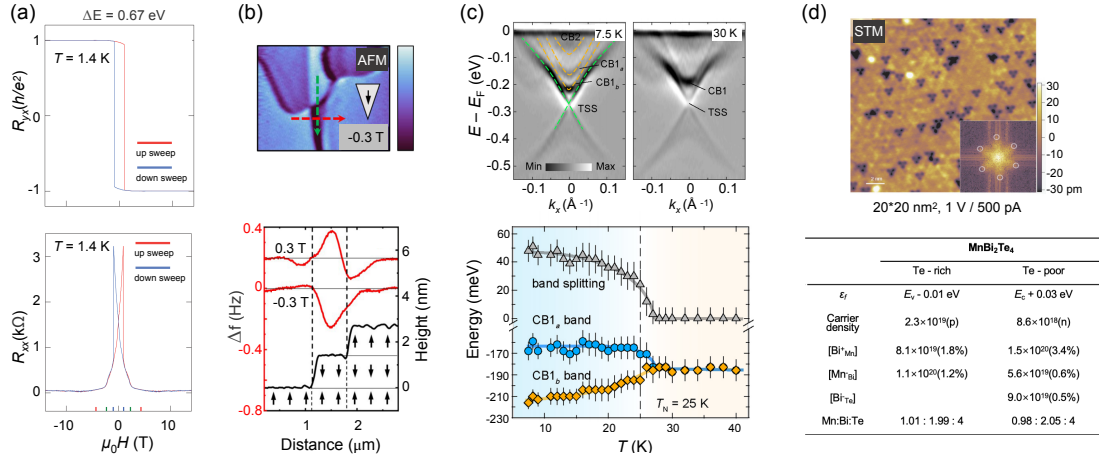


Figure 3. Key physical properties related to the gap behaviour of TSS in Mn-Bi-Te family. (a) Realization of QAHE reveals an extremely small TSS gap ($\Delta E = 0.67$ eV), from [59]. (b) Robust uniaxial A-type AFM order to the surface layers and AFM domains observed using MFM, from [91]. (c) Bulk conduction band splitting related to the AFM order as observed directly in ARPES spectra, from [48]. (d) Top panel shows two types of surface point defects (bright dots and dark triangles, probably corresponding to Bi_{Te}/Mn_{Te} and Mn_{Bi}, respectively) found in atomically resolved topographic image, from [46]; Bottom panel lists the calculated Fermi level (ϵ_f), free carrier density (and the type of the carrier), as well as densities of the most important intrinsic defects (and concentrations in atomic percent) at both Te-rich and Te-poor limits in MnBi₂Te₄, from [106].

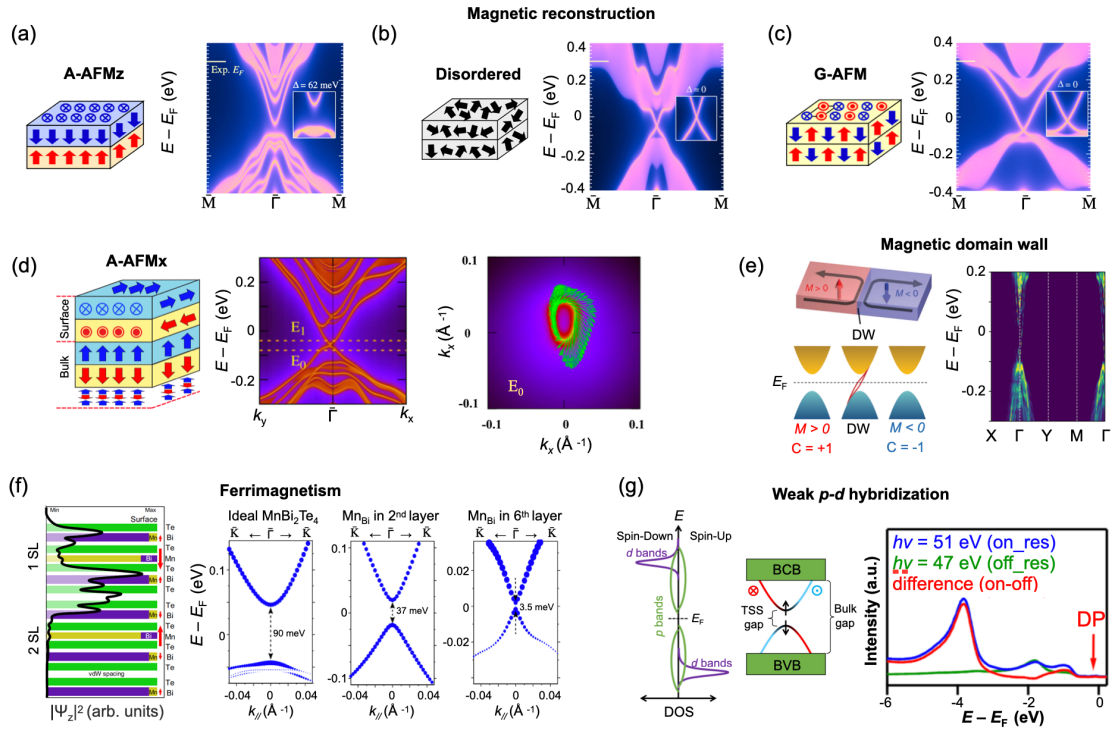


Figure 4. Various magnetic reconstructions accounting for the (nearly) gapless behavior of MnBi_2Te_4 TSSs. (a)-(c) Prototypical magnetic reconstructions leading to different gap behavior of TSS, including A-type AFM with out-of-plane FM moments (A-AFMz) (a), disordered magnetic moments (b), G-type AFM (c) (Adapted from [47]) and A-type AFM with the magnetic moments along the x -axis (A-AFMx) (d) from [107]. (e) Magnetical domain wall edge states (left, from [28]) resemble the gapless TSS, which is further discussed in a first-principles-based tight-binding model (right, from [110]). (f) Native point defects Mn_{Bi} can introduce ferrimagnetism and reduce the TSS gap, from [97]. (g) The hybridization between the Mn $3d$ and Te $5p$ states, as schematically shown in the left two panels (from [69]) is too weak according to the resonant photoemission spectra (right, from [49]) to induce TSS magnetic gap.

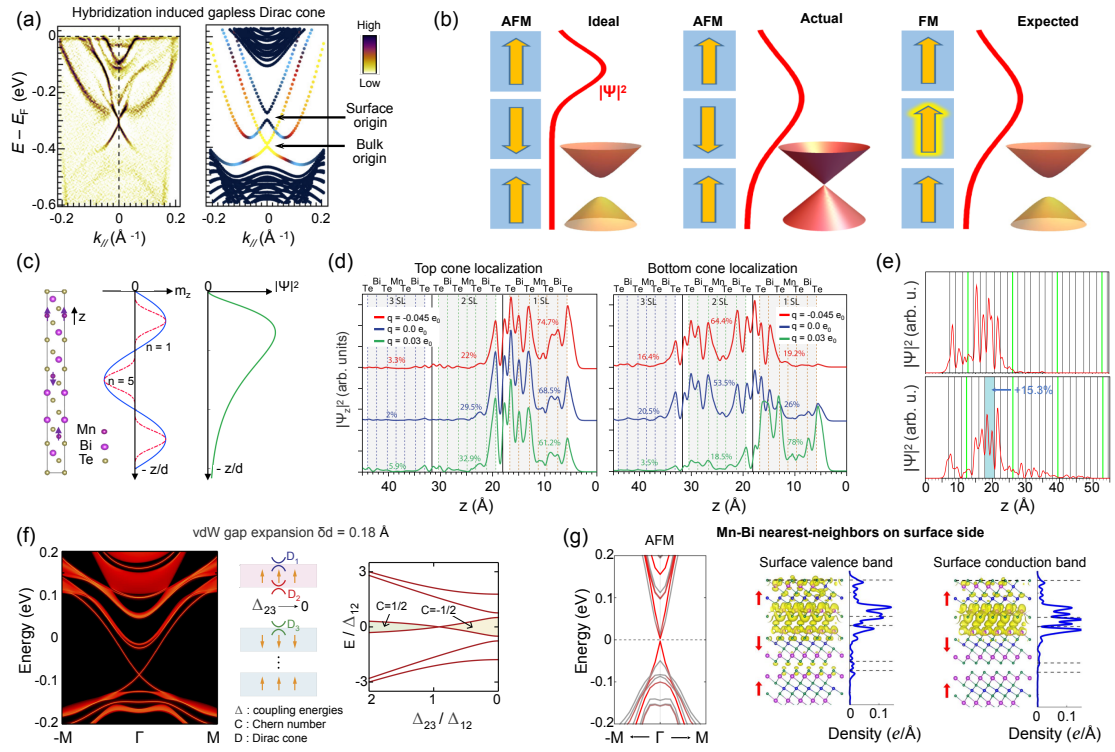


Figure 5. TSS redistribution picture explaining the (nearly) gapless behavior of MnBi₂Te₄ TSSs. (a) ARPES spectra and tight-binding model simulation show the hybridization between TSS and Rashba-split bands, from [84]. (b) Schematic showing the redistribution of TSS density of states and gapped/gapless Dirac cone corresponding to an ideal AFM phase (left), an actual AFM phase (middle) and an expected FM phase (right), from [128]. (c) Distribution of bulk magnetization (m_z) and surface state envelope function Ψ according to effective model analysis, from [111]. (d) Surface excess charge induced redistribution of TSS top/bottom cone localization, from [90]. (e) TSS redistribution due to the vdW spacing expansion, from [89]. (f) Three-Dirac-fermion approach to the gapless TSS under vdW spacing expansion, from [112]. (g) Co-antisites (exchanging Mn and Bi atoms in the surface layer) can strongly suppress the magnetic gap down to several meV in the AFM phase, from [114].

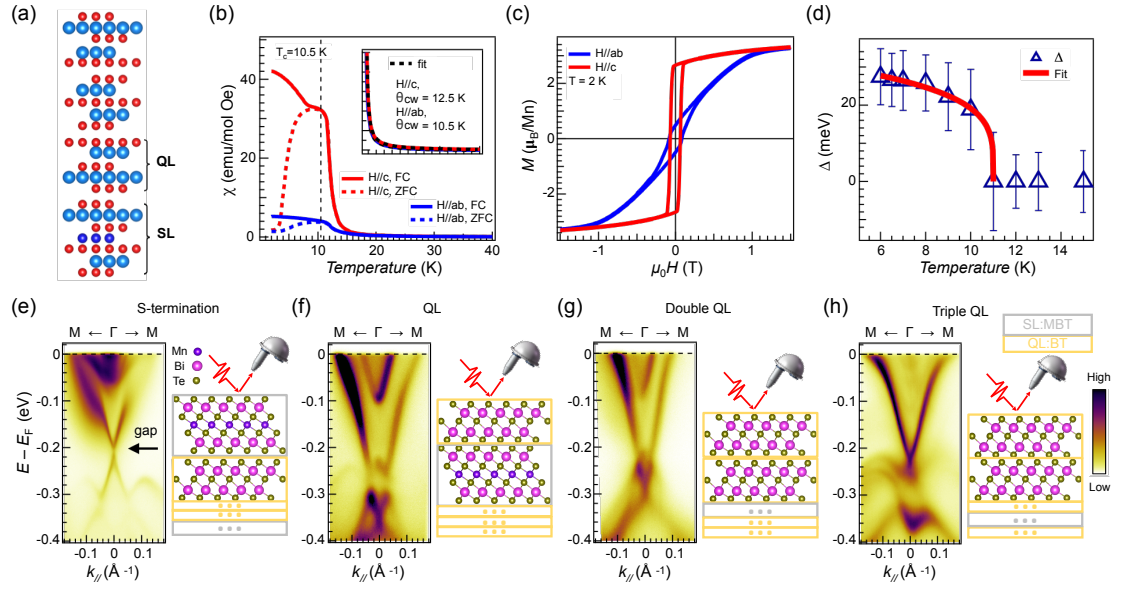


Figure 6. Realization of TSS magnetic gap from the S-termination of FM MnBi₈Te₁₃, from [120]. (a) Schematic crystal structure with one unit of -SL-QL-QL-QL- sequences. (b) magnetic susceptibility shows the FM order with Curie temperature $T_c = 10.5$ K. (c) Field-dependent magnetization hysteresis at 2 K. (d) TSS gap size vs temperature shows its FM origin. The gap size is extracted from the TSS of S-termination as shown in (e). (e-h) Termination-dependent band structure measured at 7 K in FM state. The TSS Dirac gap is indicated by a black arrow in (e).